



1 **The role of emission reductions and the meteorological**
2 **situation for air quality improvements during the COVID-19**
3 **lockdown period in Central Europe**

4 Volker Matthias¹, Markus Quante¹, Jan A. Arndt¹, Ronny Badeke¹, Lea Fink¹, Ronny Petrik¹,
5 Josefine Feldner¹, Daniel Schwarzkopf¹, Eliza-Maria Link¹, Martin O.P. Ramacher¹, Ralf
6 Wedemann¹

7 ¹Helmholtz-Zentrum Hereon, Max-Planck-Straße 1, 21502 Geesthacht, Germany

8 *Correspondence to:* Volker Matthias (volker.matthias@hereon.de)

9 **Abstract.** The lockdown measures taken to prevent a rapid spreading of the Corona virus in Europe in spring
10 2020 led to large emission reductions, particularly in road traffic and aviation. Atmospheric concentrations of NO₂
11 and PM_{2.5} were mostly reduced when compared to observations taken for the same time period in previous years,
12 however, concentration reductions may not only be caused by emission reductions but also by specific weather
13 situations.

14 In order to identify the role of emission reductions and the meteorological situation for air quality improvements
15 in Central Europe, the meteorology chemistry transport model system COSMO-CLM/CMAQ was applied to
16 Europe for the period 1 January to 30 June 2020. Emission data for 2020 was extrapolated from most recent
17 reported emission data and lockdown adjustment factors were computed from reported activity data changes, e.g.
18 google mobility reports. Meteorological factors were investigated through additional simulations with
19 meteorological data from previous years.

20 The results showed that lockdown effects varied significantly among countries and were most prominent for NO₂
21 concentrations in urban areas with two-weeks-average reductions up to 55% in the second half of March. Ozone
22 concentrations were less strongly influenced (up to +/- 15%) and showed both, increasing and decreasing
23 concentrations due to lockdown measures. This depended strongly on the meteorological situation and on the
24 NO_x/VOC emission ratio. PM_{2.5} revealed 2-12% reductions of two-weeks-average concentrations in March and
25 April, which is much less than a different weather situation could cause. Unusually low PM_{2.5} concentrations as
26 observed in Northern Central Europe were only marginally caused by lockdown effects.

27 The lockdown can be seen as a big experiment about air quality improvements that can be achieved through drastic
28 traffic emission reductions. From this investigation, it can be concluded that NO₂ concentrations can be largely
29 reduced, but effects on annual average values are small when the measures last only a few weeks. Secondary
30 pollutants like ozone and PM_{2.5} depend more strongly on weather conditions and show a limited response to
31 emission changes in single sectors.

32 **1 Introduction**

33 The global spread of the Corona virus since the start of 2020 resulted in unprecedented emission reductions caused
34 by lockdown measures in many parts of the world. In Europe, significant reductions in road and air traffic as well
35 as in industrial activities began between end of February and mid of March 2020. Emissions were heavily reduced



36 in short time, but then steadily increased again as lockdown measures were lifted step by step, until they reached
37 approximately previous year levels in summer (Forster et al., 2020). However, this temporal emission behaviour
38 varied from country to country and among the different emission sectors. Emission reductions between the second
39 half of March and end of June 2020 were probably the largest in Europe since decades, in particular in traffic.
40 From an air quality perspective, this can be regarded as a huge real world experiment about the effects of severe
41 emission reductions on air pollutant concentrations and possible side effects of emission reduction measures, e.g.
42 on secondary pollution formation.

43 Observational data at ground level and from satellite showed large, but regionally different reductions in NO₂
44 concentrations (e.g. Bauwens et al. (2020); Menut et al. (2020); Velders et al. (2021); Lonati and Riva (2021). For
45 particulate matter (PM), concentration reductions were less clear and not necessarily in line with the expectations
46 that would follow the estimated emission reductions. Obviously, also weather conditions have a significant impact
47 on pollutant concentration levels, but despite the high number of publications that analyse COVID-19 lockdown
48 effects on air pollution, meteorological influences are mostly not taken into account properly (Gkatzelis et al.,
49 2021). Wind direction determines strongly the advection of gases and aerosols from distant regions into the area
50 of interest, higher wind speeds can activate additional emission sources like re-suspension of deposited particles,
51 and precipitation amounts control deposition. In Central Europe, a period between mid of March and mid of April
52 was very sunny and dry, both conditions that favour the formation of secondary pollutants like ozone and PM and
53 that hamper particle deposition. On the other hand, advection of clean air from northern Europe influenced
54 pollution levels in northern Central Europe in the beginning of April, as well.

55 As has been pointed out in recent publications about the effect of COVID lockdown emission reductions on air
56 pollutant concentrations (e.g. Menut et al. (2020); Velders et al. (2021)), the relationship between emissions and
57 concentrations is not necessarily straightforward and easy to explain. A simple comparison between before and
58 after lockdown concentrations neglects seasonal and weather effects. A similar argument holds for comparisons
59 with the same week of the previous year. While seasonal effects are considered in this case, the weather situation
60 might still be very different. In addition, technology or economically driven emission changes from one year to
61 another are not taken into account. Chemistry transport models and sophisticated emission models can help in
62 disentangling the relationships between emissions, meteorology, and concentration levels. In addition, they can
63 quantify the contribution of different source sectors and investigate effects of reduced concentrations of specific
64 pollutants on the formation of other secondary species. For example, it has been discussed by Kroll et al. (2020)
65 and (Huang et al., 2020) that lower NO emissions might lead to higher ozone concentrations and a higher potential
66 for the oxidation of organics, which might result in increased secondary organic aerosol (SOA) formation. In fact,
67 Amouei Torkmahalleh et al. (2021) analysed observed NO₂ and O₃ concentrations in numerous cities around the
68 world and report increased ozone in urban environments. However, depending on the NO_x/VOC emission ratios
69 and the meteorological situation, the effects might differ from place to place (see e.g. Mertens et al. (2021)).

70 To quantify the effects of the lockdown measure on ambient concentrations, these need to be separated from other
71 sources of influence which predominantly are assumed to be the meteorological conditions. For Europe, Menut et
72 al. (2020) assessed the influence of lockdown measures on air quality without the biases of meteorological
73 conditions in an ad-hoc modelling study for March 2020. They compared a reference model run with 2017
74 emission data for Europe to a lockdown run with estimated emission reductions. Both runs were based on the
75 same meteorological fields. Decreases in NO₂ concentrations ranging from -30% to -50% in all western European

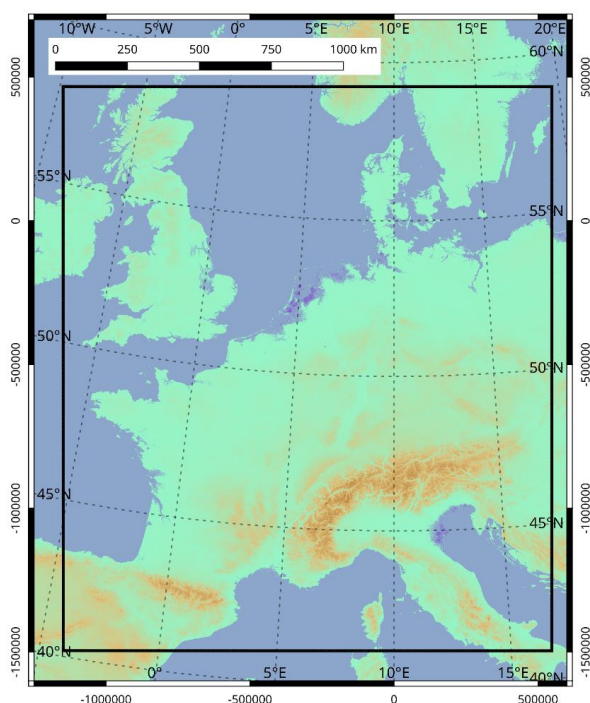


76 countries due to the lockdown measures alone have been found. The effect on fine particle concentrations has
77 been comparably less pronounced (−5 to −15%). Sharma et al. (2020) performed a similar study for India. Around
78 43%, 31%, 10%, and 18% decreases in $PM_{2.5}$, PM_{10} , CO, and NO_2 in India were observed during the lockdown
79 period compared to previous years. While, there were 17% increase in O_3 and negligible changes in SO_2 . With
80 focus on the Netherlands, Velders et al. (2021) used a machine learning (ML) algorithm (Random forest) to
81 remove the effects due to meteorological variability on pollutant concentrations. Concentrations that were
82 measured before and during the lockdown period are compared with the “expected” concentrations during this
83 period, according to the ML algorithm and the differences are ascribed to the lockdown measures. The authors
84 also applied chemical transport modelling to assess the question of separating the effects. They concluded that the
85 unusual 2020 meteorology in the Netherlands led to decreased PM_{10} and $PM_{2.5}$ concentrations by about 8% and
86 10%, respectively, but the NO_x , NO_2 , and O_3 concentrations were not affected. In a study addressing the air quality
87 during the lockdown period in Milan (Collivignarelli et al., 2020) used a different procedure based on
88 observations, only, aiming to eliminate the influence of weather phenomena on the air quality. To do so, they
89 identified a meteorological reference period in the same year around the lockdown phase. About two weeks in
90 February (7th to 20th) were considered suitable to serve as a control time segment, for which gas and particle
91 concentrations were used to quantify the lockdown effects. Using machine-learning (ML) models fed by
92 meteorological data along with other time features. Petetin et al. (2020) estimate the NO_2 mixing ratios for Spain
93 that would have been observed in the absence of the lockdown. So-called meteorology-normalized NO_2 reductions
94 induced by the lockdown measures were quantified by comparing the estimated business-as-usual values with the
95 observed NO_2 mixing ratios. It was found that the lockdown measures were responsible for a 50% reduction in
96 NO_2 levels on average over all Spanish provinces and islands during the period from 14 March to 23 April 2020.
97 Additionally, van Heerwaarden et al. (2021) used ground based and satellite observations in combination with
98 radiative transfer modelling to disentangle meteorological effects and those of aerosol emission reduction and
99 reduced contrails on observed record irradiance in Western Europe. They concluded that lockdown measures were
100 far less important for the irradiance record than the exceptionally dry and particularly cloud-free weather.

101 In this paper we present results derived with the COSMO-CLM/CMAQ model system together with a highly
102 modular emission model to quantify the contribution of the estimated emission reductions on the concentrations
103 of NO_2 , O_3 and $PM_{2.5}$ in Central Europe and to separate the contribution of emission changes from those caused
104 by distinct weather patterns. CMAQ was fed with updated emission data for the year 2020, including time profiles
105 for sectors and countries that approximate the lockdown emission reductions. Chemistry transport model
106 simulations were performed for January – June 2020. The effects of distinct weather patterns on the effects of
107 emission reductions on pollutant concentrations were investigated through additional simulations with
108 meteorological conditions for the same time period in recent previous years with very different weather conditions.
109 The results allow for an interpretation of the observed concentration reductions when compared to previous years.
110 It also gives a range of possible concentration changes resulting from the same emission reductions.



111 **2 Model simulations**



112
113 **Figure 1: Inner domain of the CMAQ model (black line) along with the coordinates of the CMAQ projection (values**
114 **outside the zebra frame)**

115 This study focuses on the effects of emission reductions during the lockdown in Central Europe in spring and
116 early summer 2020. While emission changes were considered for entire Europe, the main area under investigation
117 w.r.t. effects on concentrations covers the most populated regions in Central Europe (Fig. 1), only. This restriction
118 was applied for the sake of a higher resolution and for allowing a reasonable interpretation of meteorological
119 impacts. The Community Multi-scale Air Quality Model (CMAQ) (Byun and Schere, 2006; Byun and Ching,
120 1999) version 5.2 was used with the carbon bond 5 (CB05) photochemical mechanism (CB05tucl) (Kelly et al.,
121 2010) and the AE6 aerosol mechanism. The model was run for 2020 with a spin-up time of 2 weeks in 2019 to
122 avoid the influence of initial conditions on the modelled atmospheric concentrations. CMAQ was set up on a 36
123 x 36 km² grid for entire Europe and for a one-way nested 9 x 9 km² grid for Central Europe, see Fig. 1. The
124 vertical model extent comprises 30 layers from the model surface up to the 100 hPa pressure level. Twenty of
125 these layers are below approx. 2000 m, and the lowest layer has a height of 36 m.

126 Chemical boundary conditions for the outer model domain were taken from the IFS-CAMS analysis (Inness et al.,
127 2019b) available from the MARS archive at ECMWF and the Copernicus Atmosphere Monitoring Service
128 Atmosphere Data Store (Inness et al., 2019a). Particle and gas concentration fields of the Global Analysis and
129 Forecast are provided on a T511 spectral grid with 137 vertical levels. The IFS-CAMS data were temporally and
130 spatially remapped onto the boundary of the CMAQ domain. Finally, a unit conversion and a transformation of
131 the chemical species from IFS-CAMS to CMAQ were applied.



132 Meteorological data for the CMAQ model were provided by a simulation of the COSMO model (Baldauf et al.,
133 2011;Doms et al., 2011;Doms and Schättler, 2002) applying the version COSMO5-CLM16 (climate mode
134 (Rockel et al., 2008)). To simulate the radiative transfer as realistic as possible, an extension of the COSMO model
135 for the MACv2 transient aerosol climatology was used. The soil was initialized taking the data from a 40 year
136 simulation with the COSMO model. Then, the atmospheric simulations were performed for the period 1
137 September 2019 to 30 June 2020 using the MERRA2 Global reanalysis (Gelaro et al., 2017) as initial and lateral
138 boundary conditions. The same was done for the periods 1 September 2015 to 30 June 2016 and 1 Sep 2017 to 30
139 June 2018. To ensure that the atmospheric fields in the transient model integration are close to the observations
140 over the whole period of 10 months, a nudging technique was used as described in Petrik et al. (2021). The reader
141 is referred to this publication to find more information about the setup of the atmospheric model (setup ‘CCLM-
142 oF-SN’).

143 CMAQ simulations were performed with emissions as they could be expected for 2020 without any lockdown
144 measures and with another emission data set that was modified according to reported changes in traffic and
145 industrial activities. The latter is regarded as the emission data set that reproduces real world emissions during the
146 first COVID-19 lockdown phase in 2020 best. In the following we will refer to this simulation as the COV case,
147 while the simulations with expected emissions without lockdown is referred to as the noCOV case. The difference
148 between the simulated pollutant concentrations for the two cases represents the COVID-19 lockdown effects on
149 air quality. A detailed description of the emission data construction is given in the next section. Additional model
150 simulations with meteorological conditions for the years 2016 and 2018 have been performed with CMAQ using
151 the same 2020 emission data sets.

152 **3 Emission data**

153 **3.1 Basic emissions 2020, noCOV case**

154 Emissions are based on the CAMS-REGAP-EU version 3.1 available at the ECCAD website
155 (<https://permalink.aeris-data.fr/CAMS-REG-AP>). The dataset comprises annual totals for anthropogenic
156 emissions in 13 GNFR sectors (Granier et al., 2019). The most recent data set was for 2016. For this study, the
157 emission data was extrapolated to the year 2020 based on the temporal emission development in previous years.
158 For the application in the CMAQ model the data was re-gridded and vertically and temporally redistributed.
159 Additionally, in order to investigate the effects of lockdown measures on the emissions, sector and country specific
160 temporal profiles of lockdown effects were applied. The data preparation was done with a modular toolbox for
161 emission calculation, the Highly Modular Emission MOdel (HiMEMO), currently developed at Helmholtz-
162 Zentrum Hereon. The framework is built in the R programming language, using the libraries netcdf, proj4, sp,
163 raster and their dependencies.

164 HiMEMO was run with gridded emission data from the CAMS inventory for 2016 in a spatial resolution of 0.05°
165 $\times 0.1^\circ$. The inventory contains gridded annual emissions for chemical species groups, i.e. NO_x, NMVOC, CO,
166 NH₃, CH₄, SO₂, PM_{2.5} and PM₁₀. Several of these chemical groups need to be split into chemical components, or
167 sub-groups of species according to the CB05 chemical mechanism used by CMAQ. The NO_x split was done by
168 applying a NO/NO₂ ratio of 90/10 for traffic, a ratio of 92/8 for shipping and 95/5 for all other sectors. Land based
169 NMVOC emissions were split for individual sectors. PM was split as described by Bieser et al. (2010) for the



170 SMOKE for Europe emission model. All other species in the CAMS-REGAP-EP inventory were directly
171 transferred to CMAQ.
172 Vertical emission distributions per sector follow Bieser et al. (2011). The vertical distribution for the shipping
173 sector was treated differently for land and ocean-going ships, the latter being emitted in altitudes up to 100 m. The
174 temporal profiles follow those provided by TNO (Denier van der Gon et al. (2011), also described in Matthias et
175 al. (2018))
176 Biogenic emissions of VOCs (BVOCs) and NO were calculated with the Model of Emissions of Gases and
177 Aerosols from Nature (MEGAN) (Guenther et al., 2012). Version 3 of MEGAN (Guenther et al., 2020) was used
178 in this study, it was driven by preprocessed meteorological data for CMAQ as described above. Vegetation data
179 tables were downloaded from the MEGAN website and not further modified for this study. Leaf area index (LAI)
180 data was taken from GEOV1 products (SPOT/PROBA V LAI1) as an alternative input for MEGAN3 (Baret et
181 al., 2013).
182 The annual data for 2016 were extrapolated to 2020 for each national emission sector according to the Gridded
183 Nomenclature For Reporting (GNFR) in order to produce expected emissions for 2020 without lockdown effects.
184 The starting point were the time series data of yearly totals for the pollutants BC, CO, NH₃, NMVOC, NO_x, PM₁₀,
185 PM_{2.5} and SO₂, which are provided by the EMEP centre on emission inventories and projections (EMEP/CEIP
186 2020 Present state of emission data; <https://www.ceip.at/webdab-emission-database/reported-emissiondata>).
187 Using the time series data a mean annual change rate for emissions (CE, in %) was derived for each pollutant,
188 sector and country, separately. The projection of the 2016 emissions to the year 2020 was realized through a
189 projection factor $PF=1+CE/100*(2020-2016)$. Using a mean change rate based on the development of emissions
190 within the 3 years 2017-2019 (method 1), PF could be very large (more than 2) for some countries and sectors.
191 This can result from large changes and fluctuating time series of the yearly emissions. In order to avoid very large
192 and presumably erroneous emission changes between 2016 and 2020, a maximum allowed annual change rate
193 was introduced. If the CE was larger than 10%, a modified CE was computed by considering the entire time series
194 of annual emissions, but not more than ten years (method 2). If there still was a CE of more than 10%, we limited
195 it to a maximum change of $\pm 10\%$. Regarding the shipping sector, no changes were assumed between the years
196 2016 and 2020.

197 **3.2 Lockdown effects, COV case**

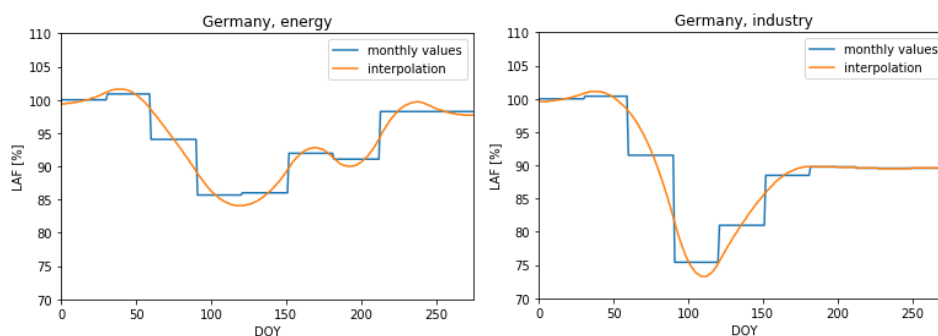
198 For the lockdown scenario, we adjusted national emissions from the following GNFR sectors: A_PublicPower,
199 B_Industry, F_RoadTransport, G_Shipping and H_Aviation. Lockdown emission reduction functions, here called
200 Lockdown Adjustment Factors (LAF) were calculated based on published data sources that resemble the effects
201 of lockdown measures on a daily basis. LAFs were derived for 42 European countries and two sea basins, the
202 North Sea and the Baltic Sea.

203 The datasets used for the construction of the modification functions are described in the following. If the input
204 data was not available for an individual country, data from a neighbouring country was used to estimate the
205 reduction. A table showing the data availability per sector and country is given in the appendix (Table A1). The
206 modification functions are applied to all species, heights and time steps of the anthropogenic emission dataset for
207 2020.

208 **A_PublicPower and B_Industry**



209 Eurostat data (https://ec.europa.eu/eurostat/databrowser/view/sts_inpr_m/default/bar?lang=en) was used to
210 account for changes in the sectors A_PublicPower and B_Industry.
211 The energy data provided there comprise monthly information on the volume index of production for electricity,
212 gas, steam and air conditioning supply. They are available for 35 countries in Europe. The industry data comprise
213 monthly information on the volume index of production for mining and quarrying; manufacturing; electricity, gas,
214 steam and air conditioning supply and construction and are available for 20 countries in Europe. The indices are
215 based on an index value of 2015. However, since we want to use them to evaluate the lockdown period, we
216 normalized the changes based on the January 2020 value. The data are given in a monthly resolution, however,
217 for many countries in Europe the lockdown started in mid of March. Therefore, a piecewise cubic spline
218 interpolation procedure was applied to derive daily lockdown adjustment factors while still maintaining the
219 monthly values. Examples are given for both sectors in Germany in Fig. 2.



220

221 **Fig. 2: Examples for monthly values and interpolated functions for Lockdown Adjustment Factors (in %) for the**
222 **sectors A_PublicPower and B_Industry in Germany.**

223 **F_RoadTransport**

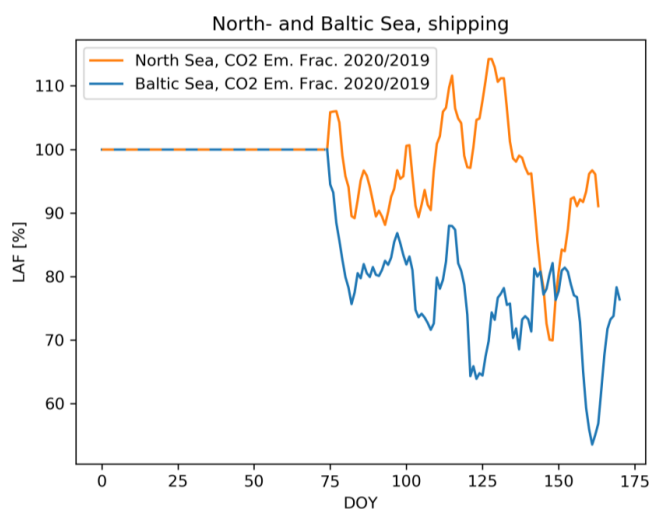
224 Google Mobility Reports (<https://www.google.com/covid19/mobility/>) deliver daily percentage change of visits
225 in different areas (e.g. residential, transit, recreation, work places). The reference value is the median of the
226 corresponding weekday between 3rd of January and 6th of February 2020. We use Google Mobility Reports for
227 transit on a national level to account for the changes in road traffic emissions. Through this method, reduced traffic
228 on national holidays, e.g. around Easter and 1 May are considered as well.

229 **G_Shipping**

230 To derive scaling factors that account for ship traffic and emission reductions in this sector, bottom-up ship
231 emission inventories were created with the HiMOSES ship emission model (Schwarzkopf et al., 2021) using
232 Automatic Identification System (AIS) data for 2019 and 2020 covering the German Bight and the Western Baltic
233 Sea. The data was recorded in Bremerhaven and Kiel by the German Federal Maritime and Hydrographic Agency
234 (BSH). A 7-days rolling mean filter was applied to the calculated CO₂ emission ratios (Figure 3). On average, the
235 data revealed a slight reduction of ship traffic in the North Sea area by approx. 10%. For the Baltic Sea traffic
236 reductions were clearly visible with a downward trend from March until mid of June that could be mainly
237 attributed to RoRo and passenger ships. For the first 75 days of the year until 15 March 2020 no reductions were



238 applied, afterwards daily LAF were used similar to the approach for road traffic. LAFs for the North Sea were
239 also applied for the Mediterranean Sea, those for the Baltic Sea were also applied to inland shipping. The reasoning
240 behind this is that shipping in the Mediterranean is mostly international cargo transport, similar to the North Sea,
241 and inland navigation is connected to short range transport, similar to the Baltic Sea. As can be seen in Fig.3
242 relative increases in shipping emissions might also occur during limited time.



243

244 **Fig 3: Lockdown adjustment factors created from the seven days rolling mean ratios of CO2 emissions from shipping**
245 **in 2020 relative to 2019. Until day 75 (15 March) no changes and a LAF of 1 was assumed.**

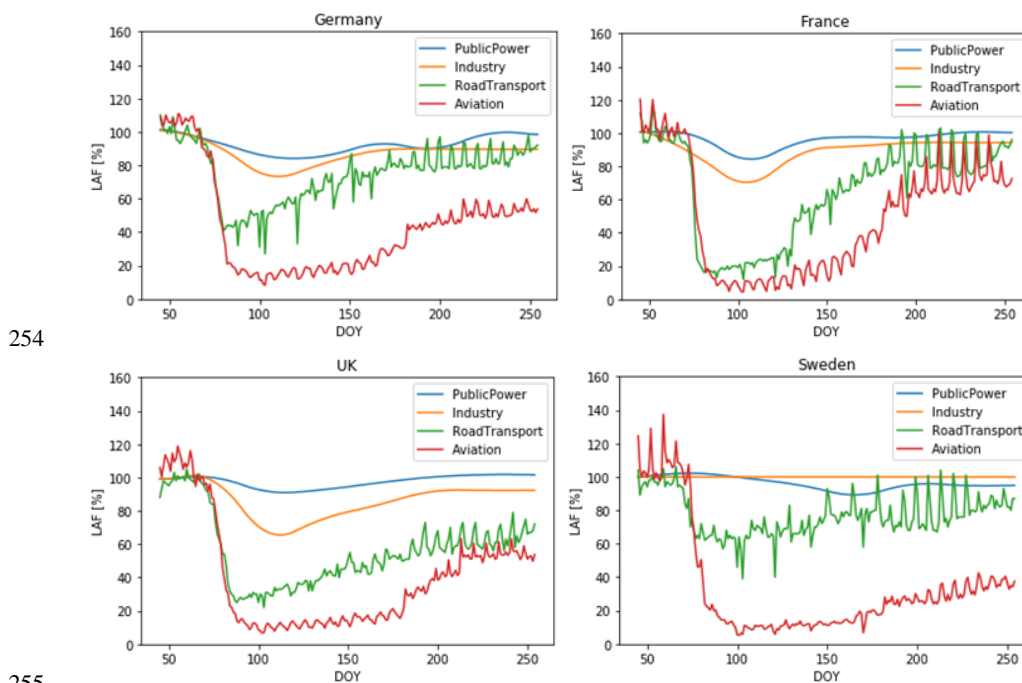
246 **H_Aviation**

247 Airport traffic total arrivals and departures data from Eurocontrol (<https://ansperformance.eu/data>) were used to
248 account for emission changes in the aviation sector. We applied a reduction based on a weekday mean from 3
249 January 2020 until 6 February 2020, similar to Google mobility data. Daily values for 42 European countries are
250 available. The relative reductions in this sector were most pronounced, reaching -90% in March and April and a
251 slower recovery than the other sectors.

252



253 **Sector Comparison**



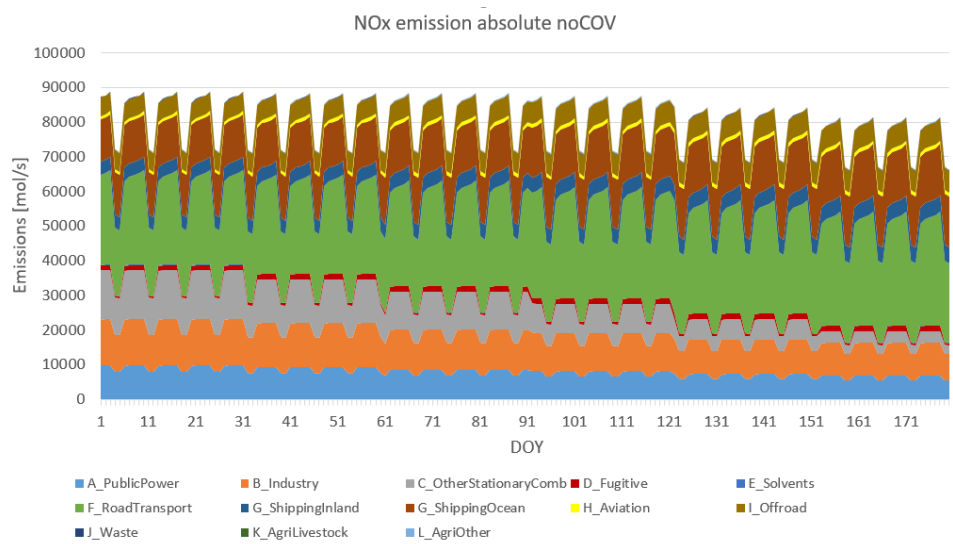
256 **Fig. 4: LAFs for Germany (a), France (b), United Kingdom (c) and Sweden (d) for the sectors: A_PublicPower,**
257 **B_Industry, F_RoadTransport, and H_Aviation**

258 LAFs for Germany, France, UK and Sweden are exemplarily shown in Figure 4. Huge emission reductions in
259 road traffic and air traffic between 10 and 20 March can clearly be seen. Public power and industry, on the other
260 hand, show much smaller reductions (10-30%) and almost reach previous year levels until the end of June. At the
261 same time in France and Germany, road traffic was back to 90% of the previous year, however in the UK and in
262 Sweden 20-40% reductions were still visible in the activity data. Comparisons of country-specific LAFs for the
263 sectors F_RoadTransport, and H_Aviation are given in the supplement (Fig. A1 and A2).

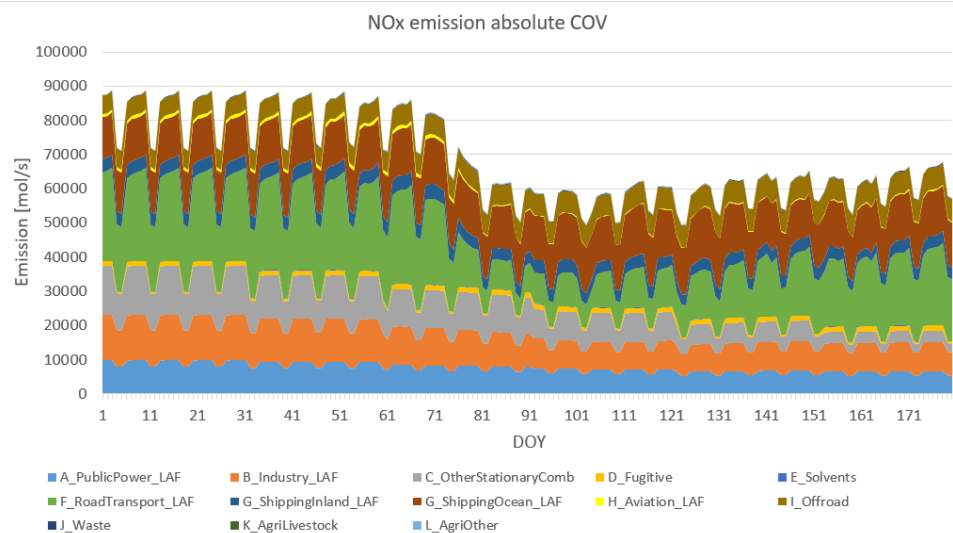
264 Figure 5 presents total daily NO_x emissions in the entire Central European domain (see Fig. 1) for the time period
265 from 1 January to 30 June 2020 for the COV and the noCOV case separated by GNFR sectors. Road transport is
266 the most important emission sector with approx. 20 to 30 %, followed by ocean shipping, other stationary
267 combustion, industry and public power, which all have similar contributions of approx. 10 %. Combustion shows
268 a clear decline towards the summer months due to the fact that domestic heating is mainly necessary in winter.
269 Reductions caused by the lockdown stem mostly from the road transport sector, with a strong drop in emissions
270 starting around day 75 (15 March). The aviation sector, which experienced the strongest relative drop in emissions
271 during the lockdown, does not play a major role for the overall emission of NO_x. However, it might be important
272 near airports and in the upper troposphere. Overall, NO_x emissions in Central Europe dropped by around 25000
273 mol/s (approx. 4 kt/h, when given as NO₂) during the strictest lockdown period in late March and early April. This
274 corresponds to a relative drop of around -30% (Fig. 5).



275



276



277

278 **Fig.5: Daily average values for sector separated NOx emissions summarized over the entire Central European model**
279 **domain for the noCOV and the COV case (with LAF).**

280 4 Observational data

281 We focus our analysis on the most important air pollutants for human health, namely NO₂, O₃ and PM_{2.5}. In this
282 chapter, first the meteorological situation between 1 January and 30 June 2020 is analysed. Afterwards,
283 observational air quality data at six selected measurement stations within the EEA network
284 (<https://www.eionet.europa.eu/countries/index>) are presented and discussed.



285 **4.1 Meteorological situation**

286 During the lockdown period in spring 2020 large parts of the region of interest experienced exceptional weather,
287 what is assumed to have a strong influence on concentrations of some of the pollutants in focus.

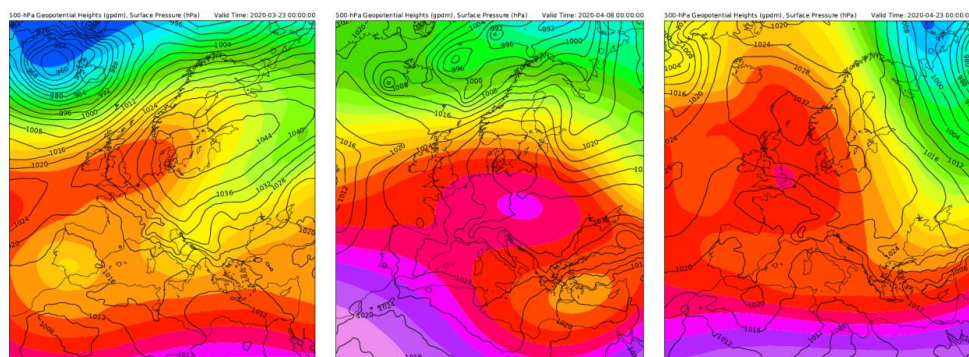
288 The weather conditions during the first half of the year 2020 show strong variations across the months and a
289 different character in the northern part of our model domain compared to more southern regions like the Po Valley.
290 While in the North February was extremely wet and windy (south-westerly direction), the second half of March
291 and April were very dry and sunny. Thus for meteorological reasons a comparison of pre-lockdown pollutant
292 concentrations with those during the lockdown is fairly meaningless in assessing the effect of corona measures on
293 the concentrations in the central and northern part of the region of interest. This appears to be different for some
294 more southerly areas, e.g. Collivignarelli et al. (2020) identified a 14 day period in February 2020 for Milan,
295 which they could use as pre-lockdown reference to evaluate emission reduction effects, since temperature, relative
296 humidity, precipitation, wind and irradiance was classified to be similar to those in March 2020.

297 To further analyse the weather regimes for the first half of 2020 the classification proposed by Hess and
298 Brezowsky (1977) has been chosen (see also Bissolli and Dittmann (2001)). This classification identifies
299 predominant synoptic regimes over Central Europe and defines 30 so called 'Großwetterlagen' (GWLs), which
300 can be isolated by an objective method introduced by James (2007). The underlying data for this analysis were
301 provided by the German Weather Service. The results of the GWL-classification can be found in supplemented
302 material, Table A2

303 **Pre-lockdown period**

304 In February 2020, an unusually wet period occurred due to strong cyclonic activity in Central Europe. Westerly
305 and North Westerly cyclonic regimes were observed on 76% of the days, whereas high pressure-type regimes
306 were observed on only 24% of the days. Thus, the shortwave downwelling irradiance in February 2020 is one of
307 the lowest measured at the weather station Wettermast Hamburg (53°31' 09"N and 10°06'10"E)
308 (<https://wettermast.uni-hamburg.de>) (Brümmer and Schultze, 2015) during the last 25 years (Figure A4), being
309 representative for north western Europe. The accumulated precipitation for February at this weather station with
310 an amount of more than 120 mm was exceptionally high compared to the last decades (Figure A4).

311



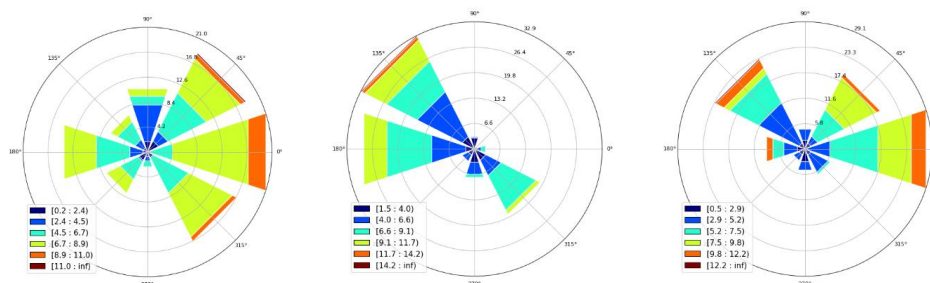
312





313 **Figure 6: 500 hPa geopotential heights (in gpdm) and surface pressure (in hPa) for selected time segments in March**
314 **and April 2020 according to the COSMO simulations. The geopotential heights are averaged over 4 days (21.03.-24.03;**
315 **6.04.-9.04., 21.04.-24.04. from left to right, respectively). Displayed surface pressure distributions are representative**
316 **snap shots within those time segments.**

317



318

319 **Figure 7: Wind roses derived from measurements of the weather station Wettermast Hamburg at an altitude of 110 m.**
320 **Results for 3 periods covering about 15 days each are shown: 16.03. – 31.03.2020; 1.04.-15.04.2020; 16.04-30.04.2020,**
321 **from left to right.**

322

323 Main lockdown period

324 For the meteorological characterisation of the main lockdown period between mid of March and end of April we
325 rely in addition to the GWL analysis on maps of the 500 hPa geopotential height and the surface pressure
326 distribution. The underlying data were extracted from simulations with the COSMO-MERRA system, the same
327 meteorological fields, which have been used for the chemistry transport calculations with CMAQ displayed and
328 discussed in the following chapters. In Figure 6 a subset of those maps for 3 selected time periods is shown; the
329 complete set of maps generated can be found in the appendix (Fig A5). To characterise and quantify horizontal
330 advection, wind roses derived from observations at the Wettermast Hamburg are displayed in Figure 7. The wind
331 data in each plot cover a time period of about 15 days. Measurements at an altitude of 110 m were chosen to better
332 represent a larger area and eliminate parts of the surface influences on the wind.

333 In mid of March, the synoptic regime substantially changed over Europe. ‘High pressure’-type GWLs became
334 dominant, i.e. high ridges over Central Europe and high-pressure systems led to a typical atmospheric blocking of
335 cyclones. The weather situation shows first a varying blocking in North- and Central Europe followed by a high
336 pressure ridge reaching from the Azores to Scandinavia (Figure 6, left), which changed to a high pressure ridge
337 stretching from Iceland into Russia. In northern Germany the wind regime was dominated by a flow with mainly
338 easterly components, which were relatively high wind speeds (Figure 7, left). In southern Europe the situation,
339 which was similar at the beginning of the period to that one in the North, changes starting about on the 23rd of
340 March, an isolated trough formed leading to low pressure system activity. For March 28 and 29 dust transport
341 from Asia and Northern Africa to the Po Valley was reported (Collivignarelli et al., 2020).

342 In the first half of April the weather in the north-eastern part of Central Europe was again quite variable, and in
343 Southern Europe the cut-off from the northern regime could still be recognized. In the western part of Central
344 Europe a ridge has established, which stretched towards the UK. Accordingly, winds in Northern Germany blew



345 predominantly from westerly/north westerly directions. Later on, a ridge over entire Central Europe dominated
346 the weather in the study domain (Figure 6, middle), only the Eastern Mediterranean was still influenced by a cut-
347 off trough. In the Po valley according to measurements around Milan, the weather during the second half of March
348 to April 10th was dry and very sunny with low to medium wind speeds (Collivignarelli et al., 2020). Towards the
349 mid of April a high pressure bridge was established reaching from Iceland into Eastern Europe.

350 In the second half of April a high pressure system established over the British Isles attached to a ridge located
351 over Central Europe leading to dry and sunny weather all over Europe. This condition was basically stable until
352 April 25th, when a cyclonic flow took over, leading to more westerly winds over Central Europe, a situation which
353 lasted until the first days of May. Winds in northern Germany switched over from easterly to more westerly
354 directions this time (Figure 7, right).

355 Overall, an exceptionally dry period occurred which started in the early lockdown period and continued until the
356 end of April. The weather was characterized by very low cloud cover and record-breaking large amounts of solar
357 irradiance (see the record at the Wettermast Hamburg in Fig. A4) and little precipitation. This exceptional weather
358 period is also discussed by van Heerwaarden et al. (2021), who reported record breaking solar irradiation for the
359 Netherlands.

360 **Lockdown transition**

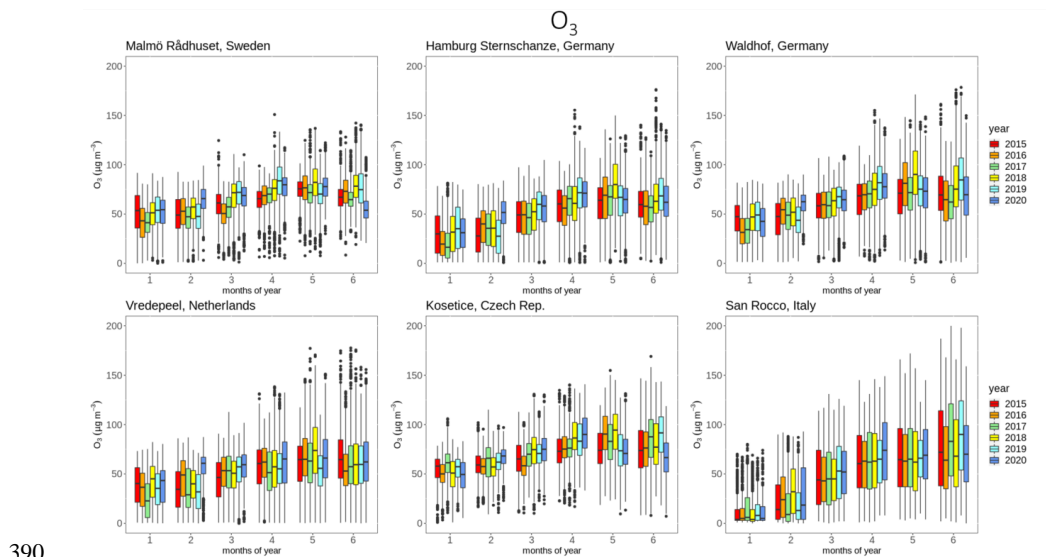
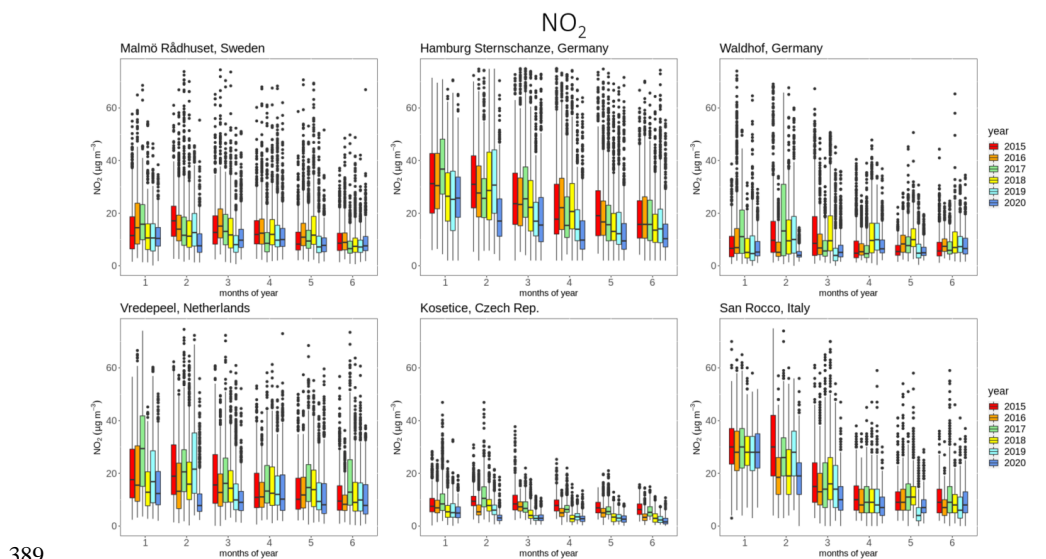
361 In May 2020, atmospheric conditions were very different in Central Europe compared to the previous months. For
362 instance, Germany was dominated by large amounts of rain in the south, sunny conditions in the west and dry but
363 cloudy conditions in the east and north. Observed sunshine duration and solar irradiance corresponds
364 approximately to average climatic conditions. In contrast, large parts of Western Europe (Netherlands, Belgium,
365 West Germany, UK) experienced sunny and dry weather throughout the entire May (van Heerwaarden et al.,
366 2021). Finally, the large scale conditions in June turned out to favour long-lasting periods with dry and sunny
367 weather conditions in Northern Germany due to blocking conditions caused by high pressure systems located over
368 Scandinavia. However, the more southerly regions were rather too wet in a climatological sense.

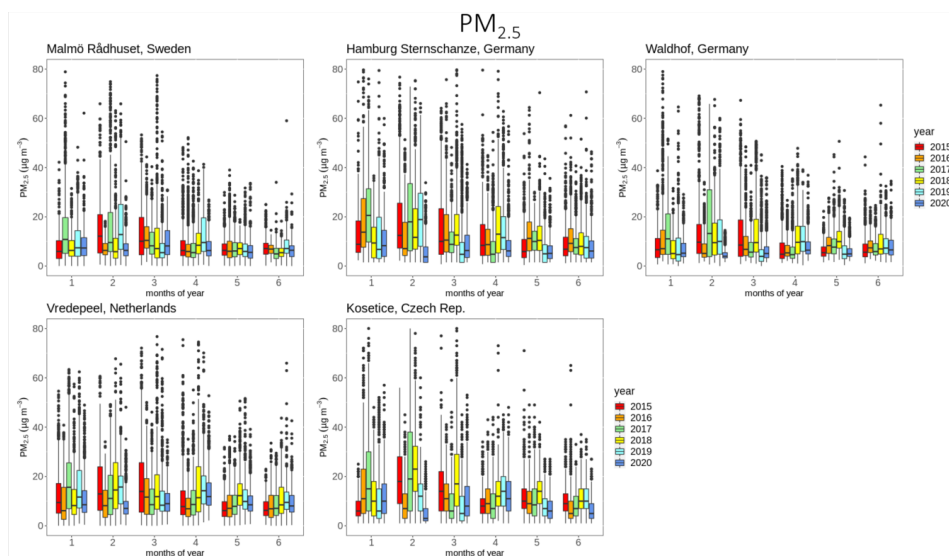
369 **4.2 Concentrations of NO₂, O₃ and PM_{2.5}**

370 The reduced emissions of pollutants during the lockdown periods, which are pronounced in certain sectors, should
371 lead to changes in ambient concentrations of those substances and related secondary pollutants as ozone. Beside
372 regional emissions also advected pollutants and the meteorological conditions determine local and regional
373 concentrations. To assess changes in air quality and alterations in the behaviour and nature of concentration time
374 series observations at selected air quality measurement stations have been examined. The analysed stations have
375 been selected in a way that they are geographically distributed over the study domain and represent different
376 emission characteristics. The stations Radhuset in Malmö, Sweden, and Sternschanze in Hamburg, Germany, are
377 classified as urban background stations, not directly influenced by traffic. In Malmö, the station is located in the
378 historical part of the town near the town hall, the Hamburg station is placed in a park of a quite lively quarter of
379 the town. Both urban background stations may be influenced by ship traffic. Waldhof is a rural background station
380 in northern Germany located about 60 km north of the city of Hannover. Vredepeel is a background station in a
381 fairly populated part of the Netherlands situated in the triangle between the cities Nijmegen, Eindhoven and Venlo.
382 The observatory Kosetice in the Czech Republic is located in the Moravian Highlands in an agricultural



383 countryside about 80 km from south-east of Prague. To represent a region south of the Alps the Italian station San
384 Rocco in Po-Valley about 30km east of Parma has been selected. With the exception of Kosetice, having an
385 elevation of about 530m, the stations are situated below an altitude of 80m. To allow a comparison of the
386 concentration measurements under different meteorological influences time series of NO_2 , O_3 , and $\text{PM}_{2.5}$ for the
387 years 2015 to 2020 have been examined. However, $\text{PM}_{2.5}$ was not available at the station San Rocco.
388





391

392 **Fig. 8: Observed monthly concentrations of NO_2 , O_3 , and $\text{PM}_{2.5}$ at Waldhof (Germany), Vredepeel (The Netherlands),**
393 **San Rocco (Italy), Kosetice (Czech Republic), Malmö (Sweden) and Hamburg (Germany). The median is displayed**
394 **within the central boxes which span from the 25th percentile to the 75th percentile, called the interquartile range of**
395 **the underlying frequency distributions. For NO_2 and $\text{PM}_{2.5}$ these distributions are based on hourly measurements at**
396 **the different stations and for O_3 on daily 8 hour maximum values. The whiskers above and below the central boxes**
397 **indicate the largest and the smallest value within 1.5 times the interquartile range, respectively. Dots denote values**
398 **outside these ranges. $\text{PM}_{2.5}$ was not available at San Rocco.**

399 The observational results for the selected stations for NO_2 , O_3 , and $\text{PM}_{2.5}$ are displayed in Fig. 8. For NO_2 , at all
400 stations, with the exception of Waldhof, an obvious trend from higher concentrations in the winter months to
401 lower ones in spring in early summer can be seen. At Waldhof this trend is not that clear due to lower values in
402 January for most of the years. As it can be expected, in urban (Malmö and Hamburg) or densely populated
403 (Vredepeel and San Rocco) regions the NO_2 concentration are on a higher level. At most stations the NO_2
404 concentrations for March 2020, the month during which in all countries the lockdown measures started, are among
405 the lowest ones compared to the previous years. For Hamburg, Vredepeel and Kosetice this also holds for the
406 months April to June. An obvious feature, which appears at all stations except San Rocco is, that the February
407 concentrations in 2020 are lower compared to the previous years, although no lockdown measures were taken in
408 Europe in February. Presumably, meteorological conditions are responsible for these relatively low NO_2
409 concentrations. February 2020 was a month with steady westerly winds and longer periods of intense precipitation
410 in Northern Europe. While strong winds cause rapid dilution of pollutants, steady precipitation has a cleaning
411 effect due dissolution of pollutants in cloud and rainwater and subsequent wash-out.

412 For O_3 , at all stations and for all years the typical trend from low winter concentrations to higher concentrations
413 in spring and early summer can be seen. During the lockdown month April the O_3 concentrations for the years
414 2018, 2019, 2020 were higher than in the previous years. During those years the radiation was rather intense in
415 April, which favours the photochemical formation of ozone. At the rural stations Waldhof and Kosetice ozone
416 concentrations in May and June 2020 were lower than in previous years. At the urban stations in Malmö and
417 Hamburg the relative increase in O_3 concentrations over the 6 month period is lower compared to the more rural
418 stations. This can be interpreted as a titration effect of O_3 by reactions with NO , which has significant sources in



419 urban areas. In general, the observations of O₃ maxima do not provide any indication of significant effects related
420 to lockdown emission changes in 2020. Possible effects of NO emission drops in March and April 2020 might be
421 low and masked by meteorological conditions.
422 PM_{2.5} concentrations also show no clear signal that would allow to relate concentrations to lockdown emission
423 reductions. Slightly higher concentrations and variability can be observed in winter compared to summer at all
424 stations. This can be related to the fact that very high PM concentrations appear in winter, only, when emissions
425 are high and atmospheric mixing is suppressed, e.g. during high pressure situations with advection of cold air.
426 Similar to the NO₂ concentrations, rainy and windy weather in February 2020 leads to low PM_{2.5} concentrations
427 at all stations

428 **5 COVID-19 lockdown effects**

429 Effects of the lockdown measures on emissions were discussed in section 3. Now, CMAQ model results are
430 evaluated for the COV and the noCOV case during the lockdown phase. Meteorological impacts are discussed
431 through comparisons of CMAQ model results that were derived with meteorological data for the years 2016 and
432 2018.

433 **5.1 CMAQ results for Central Europe**

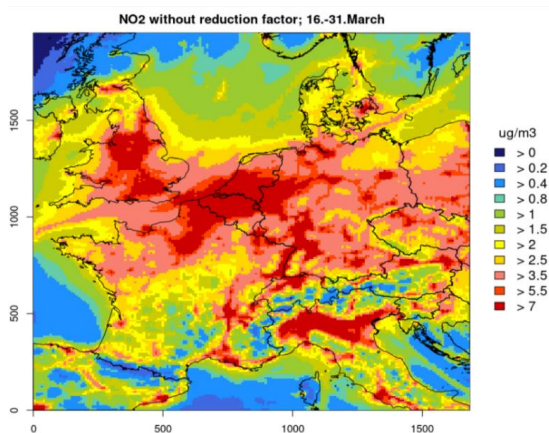
434 Differences between the CMAQ results for 2020 for the COV and the noCOV case reveal the impact of the
435 lockdown emission reductions on air pollutant concentrations. The magnitude of the concentration changes varies
436 considerably in time and space. Here, we focus our evaluation on the period with the highest emissions reductions
437 between 16 and 31 March 2020. During this time the most widely spread and temporally stable emission
438 reductions took place in Europe. Differences among weekdays and weekends and, to a limited extent, also among
439 different weather situations are averaged out by investigating a half-month-period. However, changing effects
440 over time are also discussed.

441 **NO₂ concentrations**

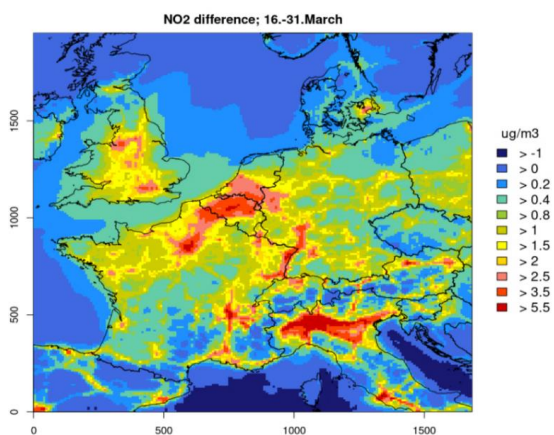
442 Figure 9 shows maps of the modelled average NO₂ concentrations in Central Europe between 16 and 31 March
443 for the case without lockdown measures (noCOV) together with the absolute and relative concentration reductions
444 caused by the lockdown. The NO₂ concentrations for the noCOV case in central Europe show the typical pattern
445 with highest concentrations in densely populated areas like England, Belgium, The Netherlands and western
446 Germany as well as northern Italy (Fig 9a). Average concentrations range between 5 and 10 µg/m³. Reductions in
447 NO₂ concentrations caused by the lockdown are highest in the same regions, also reaching several µg/m³. Relative
448 reductions are highest in France, Belgium, Italy, and Austria, reaching more than 40% on average. Germany, the
449 Netherlands, UK, southern Sweden and the Czech Republic show lower reductions between 15% and 30%. In the
450 following weeks, NO₂ concentrations stayed more or less on the same level in most parts of Europe, but the
451 lockdown effects decreased slightly as it could be expected from the emission changes. Overall, relative
452 concentration reductions were most significant in England, France, Belgium and Italy, as it was seen for the second
453 half of March. Maps for relative reductions due to the lockdown for six half-month periods between 1 March 2020
454 and 31 May 2020 are given in the appendix (Fig A6).



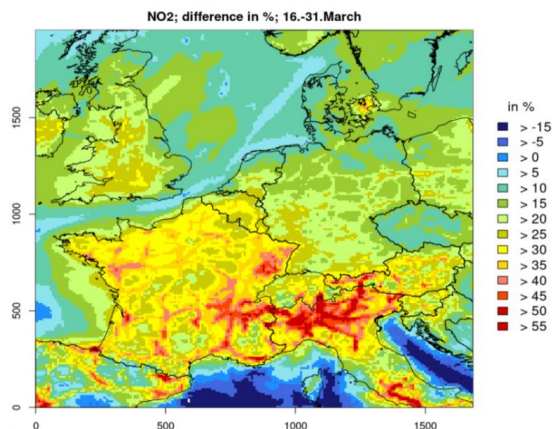
455



456



457



458 **Figure 9:** CMAQ results for NO₂ concentrations in Central Europe between 16 and 31 March 2020. Top:
459 Concentrations without lockdown measures (noCOV run). Middle: Absolute concentration reductions due to lockdown
460 measures (noCOV – COV run). Bottom: Relative concentration reductions due to lockdown measures (noCOV – COV
461 run); positive values for absolute and relative differences denote high reductions.

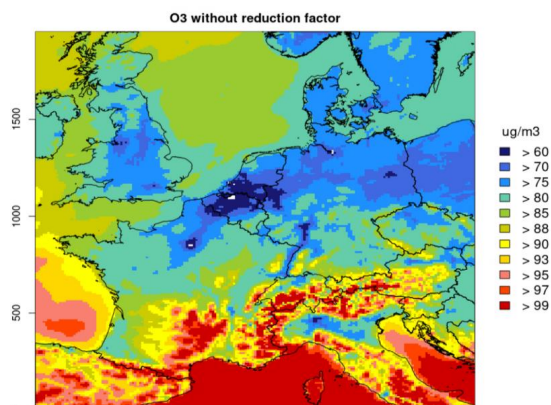


462 **O₃ concentrations**

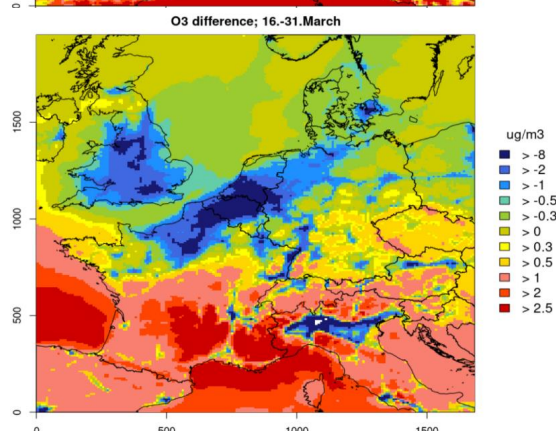
463 It can be expected that reduced NO_x emissions are also reflected in modified O₃ concentrations with lower values
464 in all regions that are NO_x-limited. However, for the second half of March increased O₃ concentrations between
465 1 and 8 μg/m³ were modelled in the COV case for northern Central Europe and the Po valley (see Fig. 10). Because
466 these are the regions with the highest NO_x emissions in Europe, they were most likely VOC-limited during this
467 first lockdown period and O₃ titration with NO was reduced when NO_x emissions were reduced. Most of the
468 southern parts of the modelling domain exhibited a decrease in ozone of 1-2 μg/m³ on average caused by the
469 lockdown and the reduced NO_x emissions. In the following weeks, areas with increased ozone turned smaller
470 week by week and were limited to large cities and the most densely populated areas, see Fig 11 for the first half
471 of April and the first half of May. Most regions in Europe turned into NO_x-limited areas in spring 2020, resulting
472 in lower ozone concentrations of 1-2 μg/m³ (about 2-4% change) caused by the emission changes during the
473 lockdown (see Fig.A7 in the supplement).



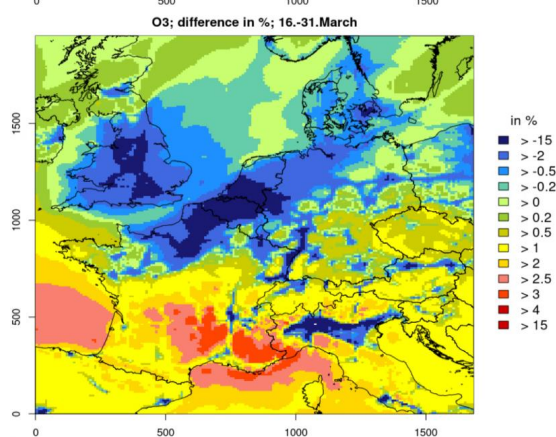
474



475



476

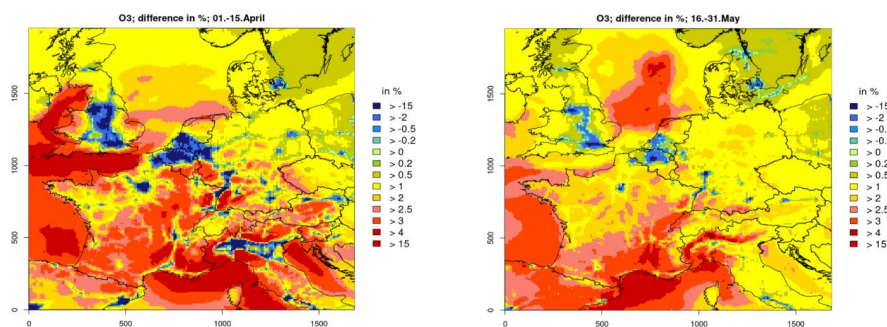


477

478 Fig. 10: CMAQ results for O₃ concentrations in Central Europe between 16 and 31 March 2020. Top: Concentrations
479 without lockdown measures (noCOV run). Middle: Absolute concentration reductions due to lockdown measures
480 (noCOV – COV run); positive values denote high reductions. Bottom: Relative concentration reductions due to
481 lockdown measures (noCOV – COV run); positive values denote reductions, negative values denote increases.



482



483

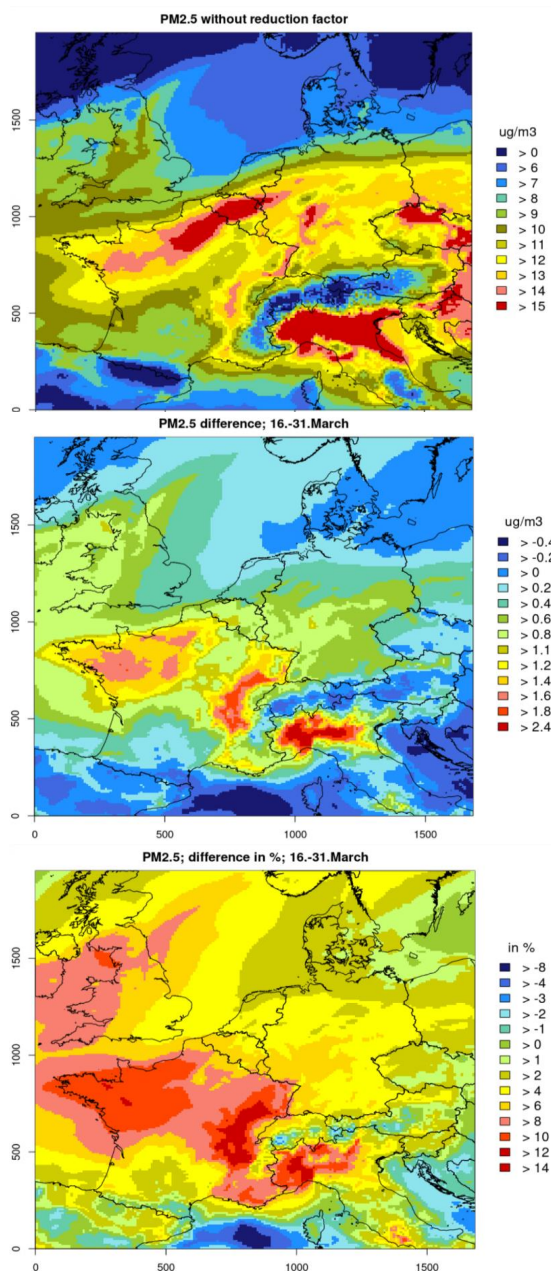
484 **Fig. 11: CMAQ results for changes in O₃ concentrations due to lockdown measures in Central Europe between 1 and**
485 **15 April 2020 (left) and 16-31 May 2020 (right). Positive values denote concentration reductions, negative values denote**
486 **concentration increases.**

487 **PM_{2.5} concentrations**

488 Simulated PM_{2.5} concentrations in the second half of March 2020 for the noCOV case show relatively high
489 concentrations between 12 and 15 $\mu\text{g}/\text{m}^3$ in large parts of Central Europe and the Po valley while the UK, Denmark
490 and Northern Germany exhibited concentrations below 10 $\mu\text{g}/\text{m}^3$ (see Fig. 12, top). The lockdown emission
491 reductions lead to concentration reductions between 1 and 3 $\mu\text{g}/\text{m}^3$ in those regions with higher concentrations
492 and values below 1 $\mu\text{g}/\text{m}^3$ in the north western part of the domain. Relative concentration decreases were most
493 significant in France and Northern Italy with values up to 20% while in the rest of the domain 6-10% lower PM_{2.5}
494 was simulated. In the following weeks, PM_{2.5} concentrations were typically reduced by 10-20% because of the
495 lockdown measures in most parts of Central Europe. Somewhat lower values were found in the Northern and
496 southern parts of the domain. The reduction in PM_{2.5} concentrations decreased to 6-12% in the second half of
497 May (see Fig. A8 in the supplement).



498



499

500

501

502 Fig. 12: CMAQ results for PM2.5 concentrations in Central Europe between 16 and 31 March 2020. Top:
503 Concentrations without lockdown measures (noCOV run). Middle: Absolute concentration reductions due to lockdown
504 measures (noCOV – COV run); positive values denote reductions. Bottom: Relative concentration reductions due to
505 lockdown measures (noCOV – COV run); positive values denote reductions.

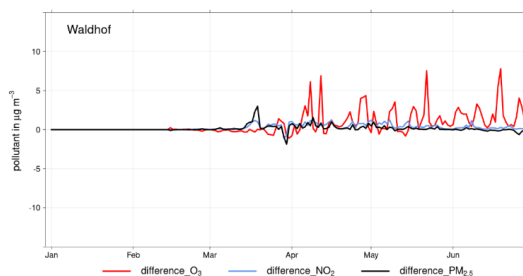


506 Temporal development of concentration changes

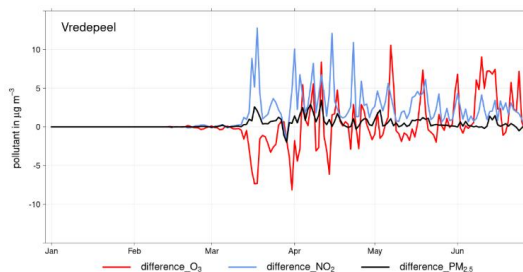
507 The detailed temporal development of the effect of lockdown emission reductions on atmospheric concentrations
508 of NO_2 , O_3 and $\text{PM}_{2.5}$ is followed at selected measurement stations. Figure 13 shows the modeled differences
509 between the noCOV and the COV model runs at Waldhof, Vredepeel, and San Rocco. Lockdown emission
510 reductions lead to reduced concentrations of NO_2 and $\text{PM}_{2.5}$ at all stations, however, the amount varies
511 considerably in time and by station. At Waldhof, only very small changes are observed. At Vredepeel, NO_2 is
512 significantly reduced (by more than $10 \mu\text{g}/\text{m}^3$ on individual days) $\text{PM}_{2.5}$ shows only small reductions. At San
513 Rocco, both, NO_2 and $\text{PM}_{2.5}$ are reduced by several $\mu\text{g}/\text{m}^3$ until the end of April. In May and June, lockdown
514 effects on the concentrations get much smaller, also at Vredepeel and San Rocco.

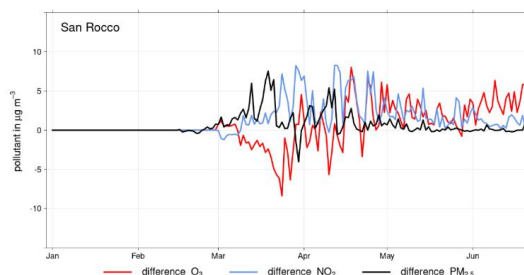
515 O_3 shows higher values despite the emission reductions until mid of April at Vredepeel and San Rocco. This is
516 because these stations are in VOC-limited areas at that time, where NO_x emission reductions lead to decreased
517 O_3 titration. This pattern changes towards end of April and in the following O_3 is decreased on most of the days
518 at all stations as a consequence of lower NO_x emissions. This effect remains variable at Vredepeel, a station close
519 to the region with highest NO_x emissions in Europe. At Waldhof, O_3 reductions are observed between beginning
520 of April and end of June. On average between 16 March and 30 June, O_3 is only decreased by $0.6 \mu\text{g}/\text{m}^3$ ($< 1\%$)
521 at Vredepeel. At Waldhof and San Rocco, the reductions are $1.2 \mu\text{g}/\text{m}^3$ (1.6%) and $1.5 \mu\text{g}/\text{m}^3$ (1.9%), respectively.

522



523





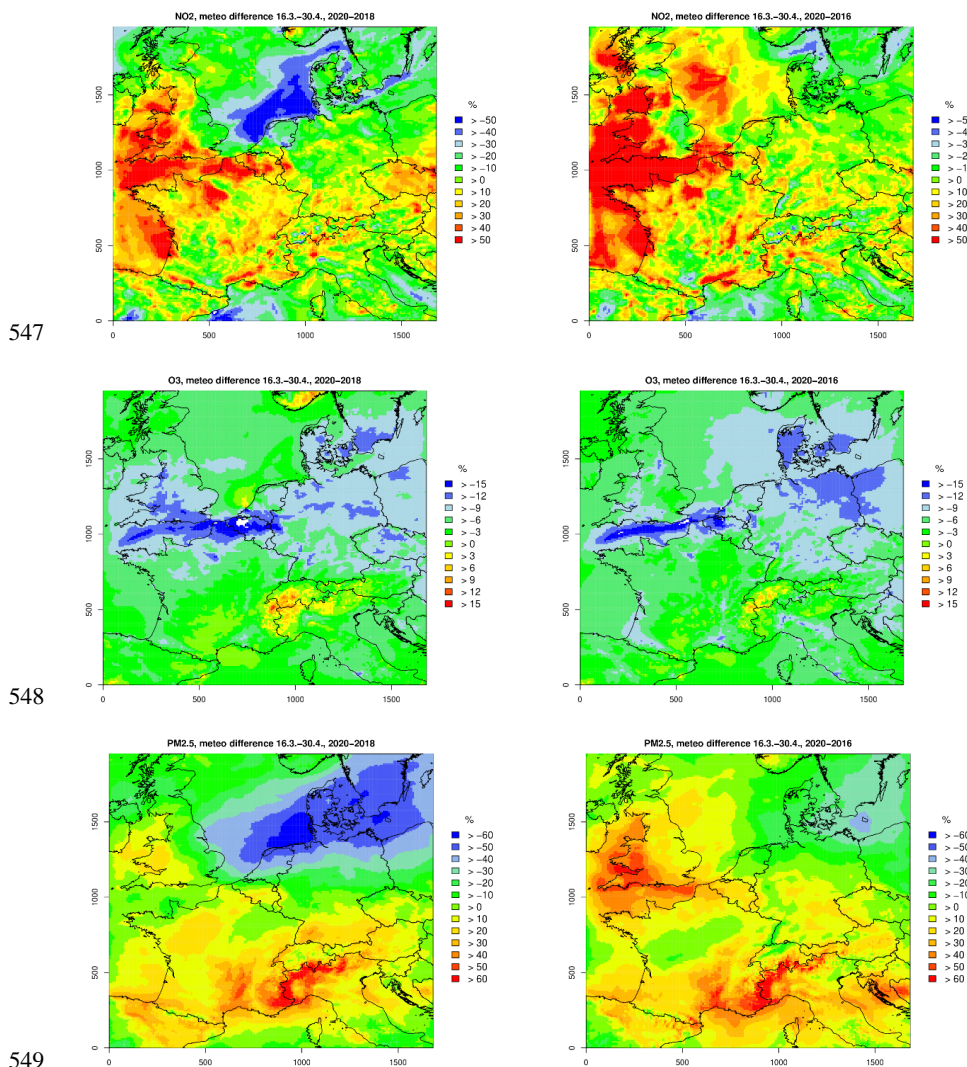
524

525 **Fig. 13: Temporal development of the differences in the simulated concentrations of O₃ (red), NO₂ (blue) and PM_{2.5}**
526 **(black) in Waldhof (top), Vredepeel (middle) and San Rocco (bottom) between 1 January and 30 June 2020.**

527 5.2 Impact of meteorological conditions

528 For investigating the effects of the exceptional meteorological situation on the concentration reductions in March
529 and April 2020, additional CMAQ model simulations were performed. Meteorological data simulated with
530 COSMO-CLM for the first six months in 2016 and 2018 was used as input data, together with the 2020 emissions
531 for both, the COV and the noCOV case. Biogenic emissions were also kept the same for the 2016 and 2018 runs
532 in order to investigate effects of meteorological conditions, only. These additional years were selected to cover a
533 span of weather situations during the lockdown phase. The selected years were different, but represent not in any
534 sense an extreme situation. They were chosen from the time span 2015 to 2019, since for these years model data
535 generated using the same advanced model settings (model version and reanalysis data) is available. The results
536 show the concentration and the changes caused by the lockdown measures as they would have happened under
537 different meteorological conditions.

538 Fig. 14, top, shows the NO₂ concentration changes for 2020 relative to 2018 and 2016 caused by meteorological
539 conditions, only, for the period between 16 March and 30 April. No emission changes because of the lockdown
540 were assumed for this investigation. Meteorological conditions in 2020 caused between 20% and more than 30%
541 lower NO₂ concentrations in large areas of the North Eastern model domain (The Netherlands, Northern Germany,
542 Denmark and Southern Sweden) compared to 2018, even without any lockdown measures. On the other hand, in
543 western UK, Belgium, Northern France, and the Czech Republic, meteorological conditions lead to 20% to more
544 than 30% higher NO₂ concentrations. The picture is similar when compared to 2016, in particular in the western
545 part of the model domain, but the area with lower NO₂ concentrations in 2020 compared to 2016 does not include
546 the North Sea and Denmark.



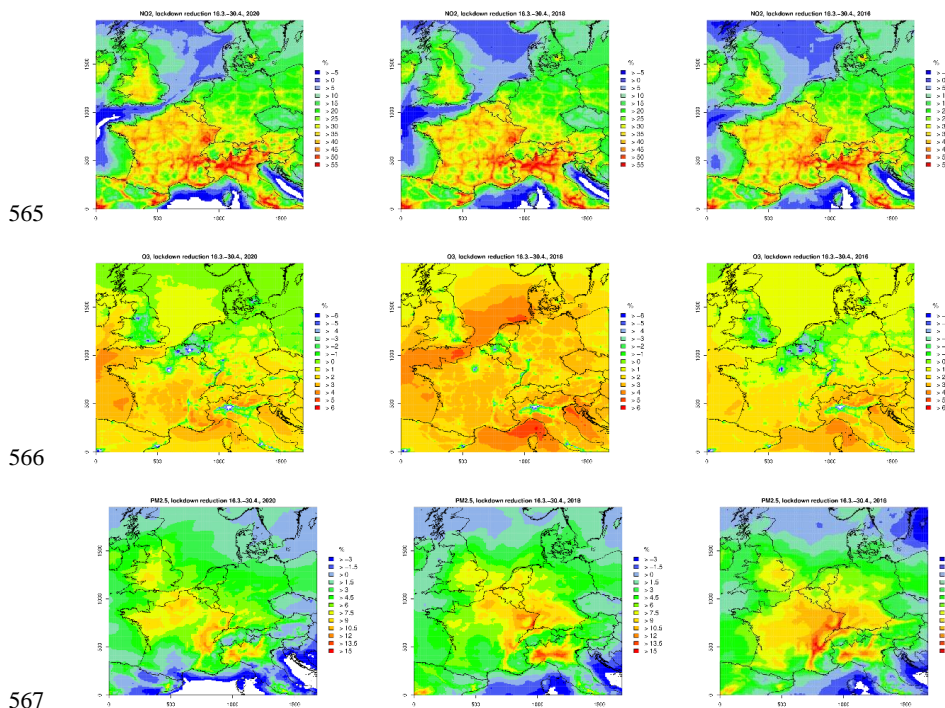
550 **Fig. 14: Relative concentration changes due to meteorological conditions in Central Europe between 16 March and 30**
551 **April simulated with CMAQ for NO₂ (top), O₃ (middle) and PM_{2.5} (bottom): The changes are represented as relative**
552 **numbers for 2020 compared to 2018 (left) and 2016 (right). Positive values denote higher concentrations in 2020 relative**
553 **to the previous year. Be aware of the different scales for each pollutant.**

554 Average ozone concentrations between 16 March and 30 April 2020 were relatively low in almost entire Central
555 Europe when compared to a situation with meteorological conditions as in 2018 and 2016 (see Fig. 12, middle).
556 Differences are in the order of 10-15% in the northern part of the model domain and between 2 and 6 % in the
557 southern part. Only in few spots in Northern Italy and Southern Switzerland, the meteorological situation in 2020
558 favoured ozone formation compared to 2016 and 2018.

559 The picture is more mixed for PM_{2.5} with considerably lower concentrations in 2020 compared to 2016 and 2018,
560 particularly in Northern Germany and Poland, i.e. in the north eastern part of the domain. Relative differences
561 reach more than 50% between 2020 and 2018 in the German Bight. Compared to 2018, PM_{2.5} concentrations were



562 also low in the western UK in 2020. In almost entire France and in Northern Italy, $PM_{2.5}$ concentrations were
563 relatively high in 2020 compared to 2016 and 2018, differences again reach more than 50% but with opposite
564 sign.



565
566
567
568 **Fig. 15: Relative concentration reductions due to lockdown measures (noCOV – COV run) in Central Europe between**
569 **16 March and 30 April simulated with CMAQ for NO_2 (top), O_3 (middle) and $PM_{2.5}$ (bottom) and three different**
570 **meteorological input data sets. Left: 2020, Middle: 2018, Right: 2016. Positive values denote concentration reductions**
571 **caused by the lockdown emission changes. Be aware of the different scales for each pollutant.**

572 The meteorological situation also affects the concentration changes caused by the lockdown, but this differs
573 considerably among the pollutants. Fig 15 shows the lockdown emission reduction effects on the average
574 concentrations for the main lockdown period from 16 March to 30 April. In most parts of Central Europe the
575 variation for NO_2 is rather small (plus/minus approx. 5%). For ozone, on the other hand, effects of the lockdown
576 are quite different among the three selected meteorological years. For 2020 meteorological conditions, relatively
577 large areas in Northern Central Europe show a slight increase in ozone (green and blue areas in Fig. 15, middle
578 row). These areas would have been smaller with 2016 meteorological conditions and limited to the most densely
579 populated areas for 2018 meteorological conditions. Lockdown effects on $PM_{2.5}$ would have been more significant
580 under meteorological conditions of the years 2016 and 2018 in almost the entire model domain (Fig. 15, bottom
581 row). Particularly in Northern Italy and South East France, changes in $PM_{2.5}$ caused by the lockdown could be
582 more than 10%, a value that was rarely reached during the real lockdown in 2020.



583 **6 Discussion**

584 **6.1 Time series at selected stations**

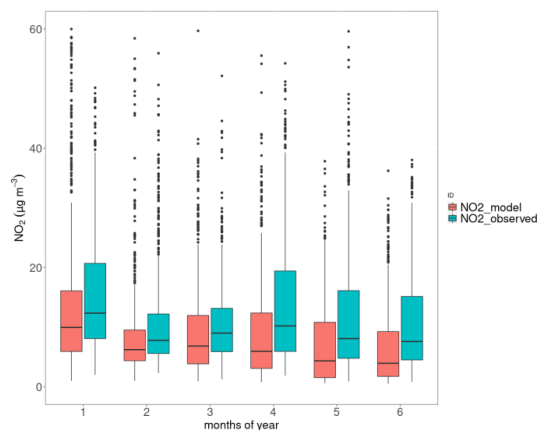
585 Observations of NO₂ and PM_{2.5} concentrations in Central Europe in the first six months of 2020 showed low
586 concentrations in March and April when compared to previous years. According to CMAQ model simulations
587 that consider lockdown emission reductions as well as emissions that could be expected for 2020, the lockdown
588 effects are strongest for NO₂ with average concentration reductions up to 40% between mid of March and mid of
589 April. PM_{2.5} shows reduction up to 20% while the effect on O₃ is much lower (up to 4% reduction). O₃
590 concentrations might even increase in large parts of northern Europe in March.

591 In order to quantify the quality of these model estimates, the simulated concentrations were compared to
592 observations at selected stations (including those presented in section 4 and 5). Figure 16 exemplarily shows the
593 comparison at Vredepeel, Table 1 contains statistical values for NO₂ and O₃ at 11 stations and for PM_{2.5} at 4
594 stations in Europe.

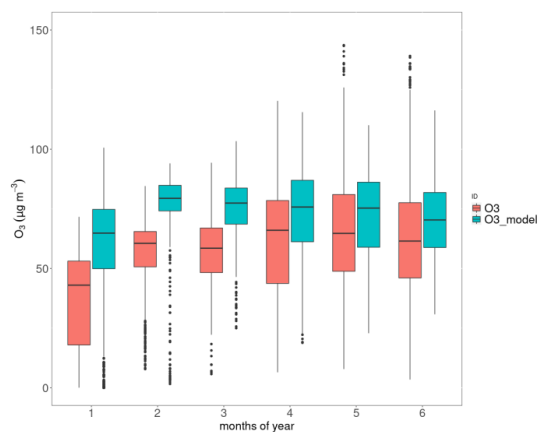
595 Modelled NO₂ concentrations are typically lower than the observed values, in particular, the model shows a
596 stronger downward trend of the concentrations in spring than observed. This pattern is reversed for ozone, where
597 the modelled 8h max concentrations are typically too high with better agreement in spring compared to winter.
598 PM_{2.5} is underestimated on average, but only at 2 out of 4 stations. Here, the agreement is typically better in winter
599 compared to spring. As average for all selected stations, the model bias for NO₂ is -17%, for O₃ it is +21% and
600 for PM_{2.5} it is -5%. The temporal correlation (R²) based on daily mean values varies between 0.42 and 0.74 for
601 NO₂, between 0.07 and 0.75 for O₃ and between 0.21 and 0.62 for PM_{2.5}. Details are given in Table 1.

602 The model is able to reproduce observed concentration levels and their spatiotemporal variation. The agreement
603 between modelled and observed concentrations is in a range that is typical for regional CTMs (see e.g. Solazzo
604 et al. (2012)). The deviations from the observed values can be interpreted as relative uncertainties in the modelled
605 lockdown effects. During the lockdown between March and June, deviations between modelled and observed
606 concentrations are often higher than the changes caused by the lockdown. Therefore, the results cannot be used to
607 judge how accurate the estimated emission reductions are.

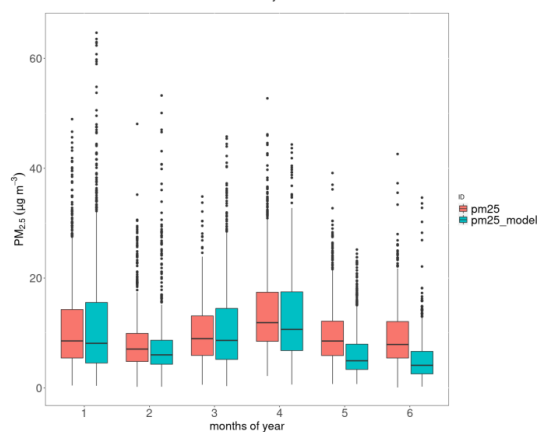
608 Based on the 6 months of simulation, the average concentrations reductions at the 11 selected stations are 14%
609 (7%-26%) for NO₂, 0.4% for O₃ (-1.3% to +1.7%) and 2.3% for PM_{2.5} (0.1% to 4.0%). While half year average
610 NO₂ concentrations in highly polluted areas decreased between 15% (Vredepeel, The Netherlands) and 25%
611 (Besenzone and Casirate d'adda, Po Valley, Italy), NO₂ reductions are much smaller (7-15%) in rural areas.
612 Average O₃ concentrations increased slightly (1%) close to cities and decreased in rural areas (up to 2%). For
613 PM_{2.5}, concentration changes at the four measurement stations were mostly between 2 and 4%. Under the
614 assumption that emission reductions were much lower in the second half of 2020, the lockdown emission
615 reductions exhibit only very small effects on annual average pollutant concentrations, especially for secondary
616 pollutants. Concentration reductions at the measurement stations for the main lockdown period (16 March – 30
617 April) are also given in Table 1.



618



619



620

621 **Fig. 16: Comparison between model results (green) and observations (red) at Vredepeel, Netherlands. Top: NO₂,**
622 **middle: O₃, bottom: PM_{2.5}. All concentrations are given in µg/m³, box plots show medians, 25% and 75% quartiles and**
623 **whiskers representing 1.5 times the interquartile range. Values that fall outside the range of the whiskers are given as**
624 **dots.**

625



626 **Table 1: Statistical evaluation of a comparison between observations of NO₂ at selected background stations of the EEA**
 627 **network with CMAQ model results between 1 Jan 2020 and 30 June 2020**

NO ₂ concentrations 1 Jan 2020 – 30 June 2020					
Station	Observed [µg/m ³]	Modelled (COV case) [µg/m ³]	Bias (model- obs) [µg/m ³]	Correlation	Lockdown effect COV-noCOV (16.3.– 30.4.) [µg/m ³]
Risoe, DK	4.7	5.7	1.0	0.46	-3.0
Waldhof, DE	5.0	3.8	-1.2	0.63	-0.6
Zingst, DE	4.4	2.9	-1.5	0.63	-0.4
Neuglobsow, DE	2.9	2.6	-0.3	0.66	-0.5
Vredepeel, NL	12.4	10.2	-2.2	0.64	-3.7
De Zilk, NL	11.4	12.8	1.4	0.51	-3.7
Kosetice, CZ	3.4	3.0	-0.3	0.42	-0.6
San Rocco, IT	13.5	9.2	-4.3	0.74	-3.7
Besenzone, IT	15.8	11.9	-3.9	0.71	-7.3
Casirate d'adda, IT	19.4	15.9	-3.5	0.71	-10.5
Paray le Fresil, FR	3.1	2.1	-1.0	0.54	-0.9
O ₃ concentrations 1 Jan 2020 – 30 June 2020					
Risoe, DK	71.2	75.7	4.5	0.07	0.5
Waldhof, DE	63.6	74.5	10.9	0.25	-0.7
Zingst, DE	70.6	79.7	9.1	0.23	-0.5
Neuglobsow, DE	62.8	74.8	12.0	0.16	-0.6
Vredepeel, NL	56.8	70.5	13.7	0.55	-0.3
De Zilk, NL	63.1	70.6	7.5	0.34	0.0
Kosetice, CZ	70.0	78.6	8.6	0.21	-1.0



San Rocco, IT	54.7	73.4	18.7	0.68	-0.9
Besenzone, IT	49.5	69.3	19.8	0.59	0.7
Casirate d'adda, IT	56.3	74.0	17.7	0.75	1.0
Paray le Fresil, FR	58.6	77.2	18.6	0.43	-1.3
PM _{2.5} concentrations 1 Jan 2020 – 30 June 2020					
Waldhof, DE	6.8	7.3	0.5	0.21	-0.1
Vredepeel, NL	10.6	9.2	-1.4	0.57	-0.4
De Zilk, NL	6.8	7.8	1.0	0.44	-0.2
Kosetice, CZ	9.3	7.8	-1.5	0.62	0.0

628

629 6.2 Emission estimates

630 Emissions for 2020 were estimated based on data for 2016 and extrapolation factors that resemble the temporal
631 development of total sectoral emissions during 3 years before 2016. This method leads to emission corrections
632 that are typically on the order of 10 % but may be up to 40%. This method bears some uncertainties, however in
633 countries that have a high share in the total emissions in Central Europe, emission trends were rather stable during
634 the last 20 years. Good agreement between observed and modelled concentrations during the weeks before the
635 lockdown gives confidence in the method.

636 Estimates for lockdown emission reductions also include several sources of uncertainty. Reduction of NO_x
637 emissions from traffic have the largest share in the emission reductions. In this approach, the LAFs applied are
638 based on google mobility data that resembles all traffic activities, regardless of their real emissions. I.e. no
639 distinction between trucks and small private cars is made and it seems likely that traffic related to transporting
640 goods was less reduced than private and commuter traffic. Therefore, emission reductions in traffic might be
641 overestimated. On the other hand, possible emission increases for residential heating that are related to more
642 people working from home were not considered at all. Small changes in other sectors like off-road machinery that
643 might have taken place weren't considered, either.

644 The cubic spline interpolation, applied to derive daily LAFs from monthly statistical data, enables to represent the
645 mean of each month correctly while giving an assumption on the daily values with a rather smooth curve. This
646 assumption does not necessarily represent the real daily conditions as extrema in the interpolation always occur
647 at the start or in the middle of the month, which might not be the case in reality. However, it is an improvement
648 compared to using monthly averages for each day of the month, as in this case, extreme jumps can occur at the
649 transition to the next month that author's assume to be more unrealistic. In addition it might resemble the rapid
650 emission reductions mid of March better than a monthly value.



651 The modelled reductions in NO₂ concentrations close to ground which are 30-40% on average during the second
652 half of March are close to what was estimated from satellite observations. (Bauwens et al., 2020) report columnar
653 NO₂ reductions of approx. 20% around Hamburg, Frankfurt and Brussels, 28% for the area around Paris and 33 –
654 38% for Northern Italy. Such values are in quite good agreement with the modelled values in this study.

655 **6.3 Impact of meteorological conditions on lockdown effects**

656 Meteorological conditions play a major role for concentrations of air pollutants. Not only emissions, but also
657 atmospheric transport and chemical transformation, as well as wet and dry deposition influence atmospheric
658 concentrations of NO₂, O₃ and PM_{2.5}. To further assess the influence of meteorological conditions on
659 concentrations of pollutants over Europe, CMAQ was run using emission data for 2020 (noCOV case) but
660 combined with meteorological input data for two different years, namely 2016 and 2018. These years were
661 selected, because they represent significantly different meteorological conditions. In the following, the differences
662 to the year 2020 for the days between 16 March and 30 April, the period that is further investigated, are briefly
663 summarized. In the supplement (Fig. A9 - A11) relevant plots showing differences for the meteorological
664 parameters 500 hPa geopotential height, total precipitation and global solar radiation can be found. The results are
665 based on the COSMO-CLM simulations for the respective years. It should be noted that the simulations for 2016
666 and 2018 do not resemble the real situation during these years, because all emissions and chemical boundary
667 conditions were for 2020.

668 **Meteorological differences 2020 versus 2016 and 2018**

669 In 2020 the geopotential height at 500 hPa over the British Isles and the North Sea was significantly higher
670 compared to that in 2016, especially from 1 April onward. This resulted in a constellation, which favours blocking
671 in 2020. Near surface high pressure systems were amplified and more persistent and weak wind conditions and a
672 more continental flow dominate. In 2016 stronger winds of Atlantic origin occasionally were observed. In 2020
673 precipitation was considerably lower compared to 2016. In most parts of the study region solar radiation was
674 clearly higher in 2020, especially over Central Europe up to the British Isles.

675 Much of what has been said concerning the blocking condition in 2020 holds as well when compared to 2018.
676 The year 2020 also was much drier and incoming solar radiation was more intense. In 2018 winds had a more
677 easterly to south-easterly component. The spatial and temporal distribution and the absolute values of the
678 meteorological parameters were slightly different in 2018 compared to 2016 (see Fig. A9- A11), so this year
679 became an additional choice for the evaluation of meteorological influences.

680 **NO₂ concentrations**

681 During the six weeks of the most stringent lockdown measures in Central Europe (16 March to 30 April), emission
682 reductions caused NO₂ concentrations reductions between 15% and more than 50%. These reductions are almost
683 independent of the meteorological situation, as can be seen in Fig 15 (top row). Differences in modelled NO₂
684 concentrations between 2020 and 2016 or 2018 show variations of more than 30%, but they are fluctuating in both
685 directions on small spatial scales (see Fig. 14, top row). Larger areas with systematic differences are mainly found
686 over sea and in areas with relatively low average concentrations, like in the western UK. It can be concluded that
687 the NO₂ concentration reductions during the lockdown were dominated by the emission reductions and not very



688 much by the meteorological situation. This is in agreement with the fact that NO_2 concentrations are spatially
689 closely connected to the emission sources. NO_2 is quickly formed from NO after the latter was emitted into the
690 atmosphere. It will then react further to form O_3 at daytime. Compared to O_3 and secondary PM, NO_2 is a rather
691 short-lived gas with high spatial gradients and a clear annual cycle. However, as the situation in February 2020
692 shows, very unusual meteorological conditions, can also cause large deviations from expected concentrations.

693 **O_3 concentrations**

694 Ozone concentrations depend more strongly on weather conditions and on emissions of other precursors like
695 VOCs. Therefore, meteorological variations from year to year might have a much stronger influence on average
696 concentrations than the emission reductions during the lockdown. The six-weeks-average ozone concentrations
697 vary by +/- 15% between 2020 and 2016 or 2018 (Fig 14, middle row) while the lockdown effects are mostly in
698 the range of +/- 5% (Fig 15, middle row), except in densely populated areas. Weather conditions between 16
699 March and 30 April 2020 favoured relatively lower ozone concentrations in most parts of Central Europe when
700 compared to 2016 and 2018. In the simulations, only areas in the western Alpine region show higher ozone in
701 2020 (Fig 14, middle row). First of all, this is surprising because 2020 was comparably sunny and dry, which
702 should favour ozone formation. However, advection of relatively clean air from Scandinavia into the North
703 Eastern part of the model domain led to lower ozone concentrations particularly in the second half of April. A
704 comparison of the meteorological effects on NO_2 and O_3 in Fig 14 also shows that NO_2 was relatively high and
705 O_3 relatively low in 2020 in the English Channel, in south western UK and Belgium. The high pressure situation
706 with relatively low wind speeds in 2020 resulted in efficient ozone destruction at night in areas with high NO
707 emissions.

708 Lockdown emission reductions caused relative ozone increases in urban areas and throughout the northern part of
709 the model domain, because these areas are VOC-limited regions. For northern Central Europe this is connected
710 with advection of clean air from north east. Lockdown effects on ozone might differ in sign under different
711 meteorological conditions, as can be seen in Fig 15. About 2-4% O_3 concentration reductions in most parts of
712 Central Europe could have been expected with 2018 meteorological fields, when solar radiation was lower but
713 more southerly winds prevailed in northern Central Europe. On the other hand, with 2016 meteorological
714 conditions ozone changes would show similar patterns as 2020. Ozone chemistry depends on radiation,
715 precipitation, atmospheric mixing and the availability of precursors in a complex way. The response of ozone
716 concentrations to emission changes is therefore not straightforward to predict.

717 **$\text{PM}_{2.5}$ concentrations**

718 $\text{PM}_{2.5}$ is another secondary pollutant that depends strongly on weather conditions, but emission reductions will
719 primarily lead to concentration reductions (see Figures 12 and 13). However, the strength of this effect might also
720 vary considerably with meteorological conditions. Fig 14 (bottom row) shows that the main lockdown period in
721 2020 was favourable for $\text{PM}_{2.5}$ formation in most parts of Central Europe, with often 20% to 50% higher $\text{PM}_{2.5}$
722 concentrations compared to other meteorological situations. An exception is the north eastern part of the model
723 domain, where the meteorological situation in 2020 led to much lower $\text{PM}_{2.5}$ concentrations compared to 2018
724 (more than 50% lower) and 2016 (20-40% lower). Similar to the situation for ozone, this is connected to the
725 easterly and north easterly winds and the advection of clean air. Consequently, lockdown emission reductions had



726 only very minor effects on $PM_{2.5}$ concentrations in 2020 in southern Sweden, Denmark, Poland and northern
727 Germany. Higher $PM_{2.5}$ reductions would have been observed in most parts of Europe with 2016 and 2018
728 meteorological conditions. This can be interpreted in a way that the main lockdown period in 2020 was favourable
729 for $PM_{2.5}$ formation in large parts of Europe leading to smaller relative $PM_{2.5}$ concentration reductions, given that
730 the emission changes are the same.

731 Summarized, it can be said that the effects of lockdown emission reductions depend strongly on the meteorological
732 situation and that concentration changes because of weather conditions might be stronger than those of large
733 emission changes during a six weeks period in spring. However, this mainly holds for the secondary pollutants O_3
734 and $PM_{2.5}$, while the effects on NO_2 concentrations are less pronounced. Particularly changes in O_3 concentrations
735 are difficult to predict because of the complex emission-chemistry-meteorology interactions.

736 **7 Conclusions**

737 In this study, emission reductions during the first and most significant lockdown phase in Europe are estimated
738 from available mobility data, AIS ship position data and statistical data about industrial production and energy
739 use. They are applied to European emission data that is updated for 2020 following recent emission trends in
740 individual countries and sectors. Through meteorological and chemistry transport modelling with the COSMO-
741 CLM/CMAQ model system for Europe, and in higher spatial resolution for Central Europe, lockdown effects on
742 air pollutant concentrations are calculated. These are put into perspective with available observational data and
743 with modelled concentration changes from year to year that can be caused by varying meteorological conditions
744 for the same time of the year. The following conclusions can be drawn from this investigation.

745 Lockdown emission reductions in spring 2020 in Central Europe are significant, in particular those in traffic.
746 Other sectors, like shipping, might be of regional importance, but emission changes for this sector are less certain.
747 Aviation shows the largest relative reduction among the emission sectors considered, however the contribution to
748 the total emissions reductions is small because of its low share in total NO_x emissions. Consequently, strongest
749 lockdown emissions reductions are seen for cities. The period with largely reduced emissions was limited to a few
750 weeks and emissions increased again towards mid of 2020.

751 In absolute numbers, concentration reductions are strongest for NO_2 in cities and for larger areas in the Po valley
752 with more than $6 \mu\text{g}/\text{m}^3$ for a two weeks average in the second half of March. Northern Italy also shows the
753 strongest relative decline with more than 50%. Rural areas in Germany, Poland and the Czech Republic show the
754 lowest reductions between 10% and 20%.

755 Ozone concentrations were often reduced, but not in cities and not in northern Europe between mid of March and
756 beginning of April. This can be explained by reduced titration in cities ($NO - O_3$ reactions that destroy ozone)
757 during the first phase of the lockdown, when NO emissions were lowest. However, when VOC emissions increase
758 in spring, most regions turn into NO_x -limited areas, which means that ozone concentrations also decrease when
759 NO_x emissions decrease. The O_3 concentration changes are around $\pm 5\%$ which is much less than the NO_2
760 changes. The impacts of meteorological conditions can be much larger and the temporary O_3 increase in north
761 east Europe in March would not have taken place under meteorological conditions as they were present in the
762 years 2016 and 2018.

763 $PM_{2.5}$ concentrations are also decreased because of the lockdown emissions reductions, but the magnitude is much
764 smaller than for NO_2 , only between 2-10 %. Again, concentration changes can be much larger due to



765 meteorological conditions. The reductions in 2020 were relatively lower compared to the effects with 2016 and
766 2018 meteorological conditions.

767 Because the meteorological effects on concentrations of O₃ and PM_{2.5} are larger than the lockdown emission
768 reduction effects, it is difficult to judge or even quantify emission reduction effects by observations and
769 comparison with previous years, only. For NO₂, this is different, but in exceptional situations, like in February
770 2020, NO₂ can also be strongly influenced by meteorological conditions and lead to lower concentrations than in
771 March during lockdown conditions.

772 Meteorological and chemistry transport models need to be applied to investigate the effects of emission reductions
773 and separate them from meteorological effects. Although these models have deficiencies and systematic errors,
774 e.g. underestimation of NO₂ and PM_{2.5} concentrations, the impacts of emission changes caused by the lockdown
775 can be quantified. The effects in absolute numbers might be lower by the same magnitude as the model
776 underestimates NO₂ and PM_{2.5}. The model accuracy is not sufficient to judge the correctness of the emission
777 reduction estimates, however, the calculated NO₂ reductions agree well with estimations from ground based and
778 satellite observations for Central Europe.

779 The emission reductions for several weeks during the first COVID-19 lockdown in Europe were the largest since
780 decades. They can be seen as a huge test for emission reductions that could be achieved with significantly reduced
781 car traffic and air traffic. The reductions resulted in much lower NO₂ concentrations, particularly in cities, but the
782 effects on secondary pollutants like ozone and PM_{2.5} were limited and are hard to predict. The latter holds
783 particularly for ozone that might even increase in some areas when traffic emissions are decreased. Year-to-year
784 variability caused by meteorological conditions has larger impacts on O₃ and PM_{2.5} than the lockdown emission
785 changes. This implies that systematic changes in prevailing weather situations that might appear due to climate
786 change could mask effects of emission reductions on secondary pollutants. The relatively short duration of strong
787 lockdown measures also results in limited effects on annual average NO₂ concentrations. Depending on location,
788 only between 3% and 15% lower values could be reached.

789 **Acknowledgements**

790 The Community Air Quality Modeling System (CMAQ) is developed and maintained by the US EPA. Its use is
791 gratefully acknowledged.

792 We thank to the weather mast group of the Meteorological Institute at the University of Hamburg, who delivered
793 data from tower site Wettermast Hamburg.

794 We also thank the German Maritime and Hydrographic Agency for supporting us with AIS data taken in
795 Bremerhaven, Hamburg and Kiel.

796 **Author contribution**

797 VM developed the idea, designed and supervised the study, evaluated part of the model results, prepared the
798 manuscript and wrote most of the text. MQ co-designed the study, wrote most of the text about the meteorological
799 situation and provided interpretations of the meteorology-chemistry interactions. JAA helped in designing the
800 study, performed CMAQ model runs and provided code for the emission data preparation. RB developed the
801 Lockdown Adjustment Factors, extrapolated emission data, and wrote the section about the emission data. LF



802 performed CMAQ model runs, evaluated CMAQ model results and observation data and provided most of the
 803 plots. RP performed COSMO model runs, provided information for the meteorological data interpretation, wrote
 804 the text about the COSMO setup and part of the text about the meteorological situation, and analysed COSMO
 805 model results. JF developed emission extrapolation factors, and provided interpretation of the observational data.
 806 DS analysed AIS data and calculated ship emission LAFs. EML collected and analysed observational data and
 807 provided data interpretation. MR helped in designing the study, analysed and interpreted observational data for
 808 suburban stations. RW collected data on aviation emissions, provided LAFs for aviation and contributed to the
 809 discussion of the results

810 **Appendix A**

811 **A1 Emission data**

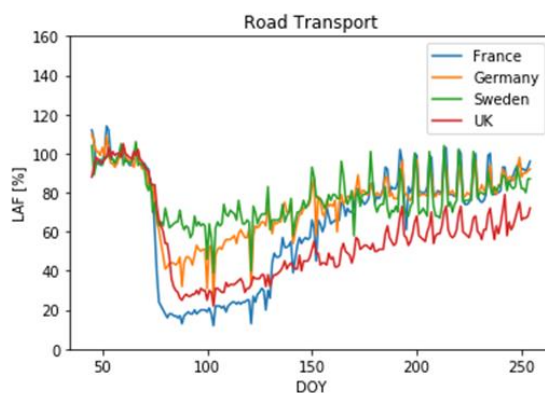
812 **Table A1: Overview on available emission reduction information for countries in the investigated domain during the**
 813 **lockdown applied in this study**

Country or Ocean Area	A_PublicPower	B_Industry	F_RoadTransport	G_Shipping	G_Shipping_Inland	H_Aviation
Albania					x	x
Austria	x	x	x		x	x
Baltic Sea				x		
Belarus			x		x	x
Belgium	x	x	x		x	x
Bosnia and Herzegovina	x		x		x	x
Bulgaria	x	x	x		x	x
Croatia	x	x	x		x	x
Cyprus	x				x	x
Czech Republic	x	x	x		x	x
Denmark	x	x	x		x	x
Estonia	x		x		x	x
Finland	x	x	x		x	x
France	x	x	x		x	x
Germany	x	x	x		x	x
Greece	x		x		x	x
Hungary	x	x	x		x	x
Iceland					x	x
Ireland	x		x		x	x
Italy	x	x	x		x	x
Latvia	x		x		x	x



Liechtenstein			x		x	
Lithuania	x		x		x	x
Luxembourg	x	x	x		x	x
Malta	x		x		x	x
Moldova			x		x	x
Montenegro	x				x	x
Netherlands	x	x	x		x	x
North Macedonia	x		x		x	x
North Sea				x		
Norway	x		x		x	x
Poland	x	x	x		x	x
Portugal	x	x	x		x	x
Romania	x	x	x		x	x
Russia			x		x	x
Serbia	x		x		x	x
Slovakia	x	x	x		x	x
Slovenia	x	x	x		x	x
Spain	x	x	x		x	x
Sweden	x		x		x	x
Switzerland	x		x		x	x
Turkey	x		x		x	x
United Kingdom	x	x	x		x	x
Ukraine			x		x	x

814

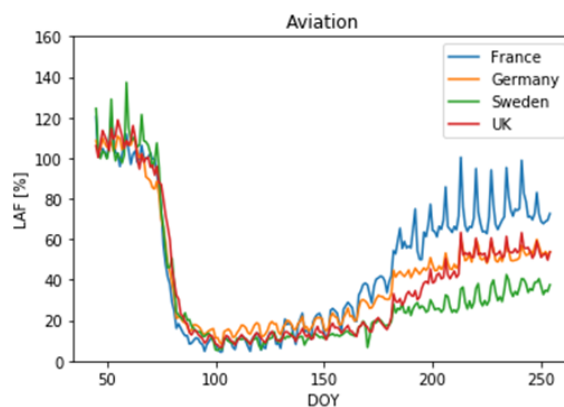


815

816 **Figure A1: Daily values for Lockdown Adjustment Factors (in %) for the sector F_RoadTransport based on transit**
 817 **data from the Google Mobility Reports.**



818



819

820 **Figure A2: Daily values for Lockdown Adjustment Factors (in %) for the sector H_Aviation based on Eurocontrol**
 821 **data.**

822 **A2 Meteorological situation**

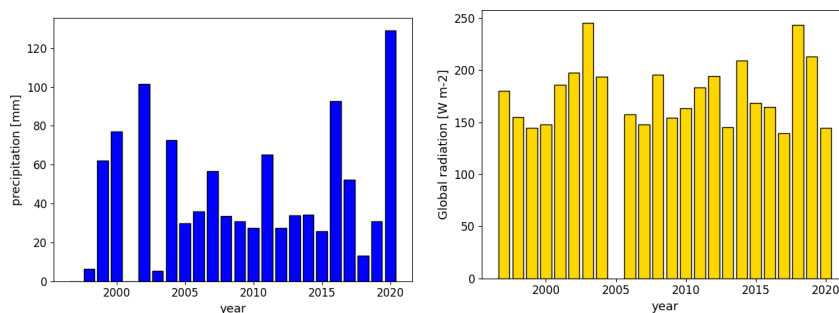
823 **Table A2: GWL classification for the period 1 February 2020 – 31 May 2020**

Date range	GWL
01.02. - 02.02.	Cyclonic Westerly
03.02. - 05.02.	Cyclonic North-Westerly
06.02. - 08.02.	High over Central Europe
09.02. - 12.02.	Cyclonic Westerly
13.02. - 16.02.	Anticyclonic South-Westerly
17.02. - 25.02.	Cyclonic Westerly
26.02. - 28.02.	Cyclonic North-Westerly
29.02. - 03.03.	Trough over Western Europe
04.03. - 06.03.	South-Shifted Westerly
07.03. - 09.03.	Maritime Westerly (Block E. Europe)
10.03. - 12.03.	Cyclonic Westerly
13.03. - 16.03.	Zonal Ridge across Central Europe
17.03. - 20.03.	Anticyclonic Westerly
21.03. - 26.03.	Scandinavian High Ridge C. Europe
27.03. - 29.03.	Anticyclonic North-Easterly
30.03. - 01.04.	Anticyclonic Northerly
02.04. - 04.04.	Anticyclonic North-Westerly
05.04. - 08.04.	Anticyclonic Southerly
09.04. - 11.04.	High over Central Europe
12.04.	undefined
13.04. - 15.04.	High over the British Isles
16.04. - 18.04.	Icelandic High Ridge C. Europe
19.04. - 23.04.	High Scandinavia-Iceland Ridge C. Europe
24.04. - 26.04.	Anticyclonic North-Westerly



27.04. - 29.04.	South-Shifted Westerly
30.04. - 02.05.	Cyclonic Westerly
03.05. - 05.05.	Anticyclonic Northerly
06.05. - 08.05.	High over Central Europe
09.05. - 12.05.	Icelandic High Trough C. Europe
13.05. - 15.05.	Anticyclonic North-Westerly
16.05. - 18.05.	Zonal Ridge across Central Europe
19.05. - 23.05.	High over Central Europe
24.05. - 27.05.	Anticyclonic Northerly
28.05. - 30.05.	Anticyclonic North-Easterly
31.05. - 02.06.	High Scandinavia-Iceland Ridge C. Europe

824



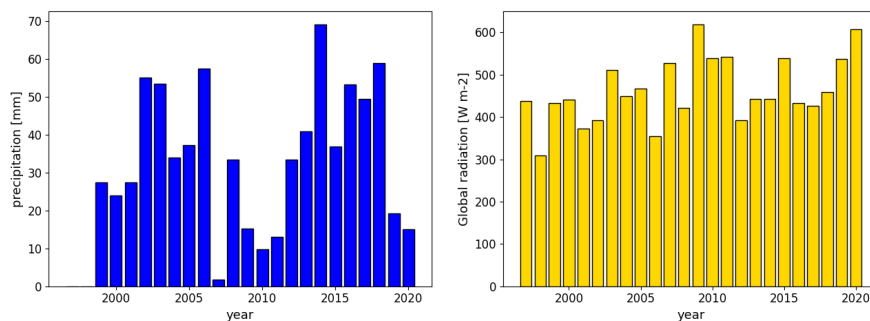
825

826

827

Figure A3: Time series of the monthly accumulated precipitation and mean solar irradiance between 10 and 14 UTC at the Wettermast Hamburg for February from 1997-2020.

828



829

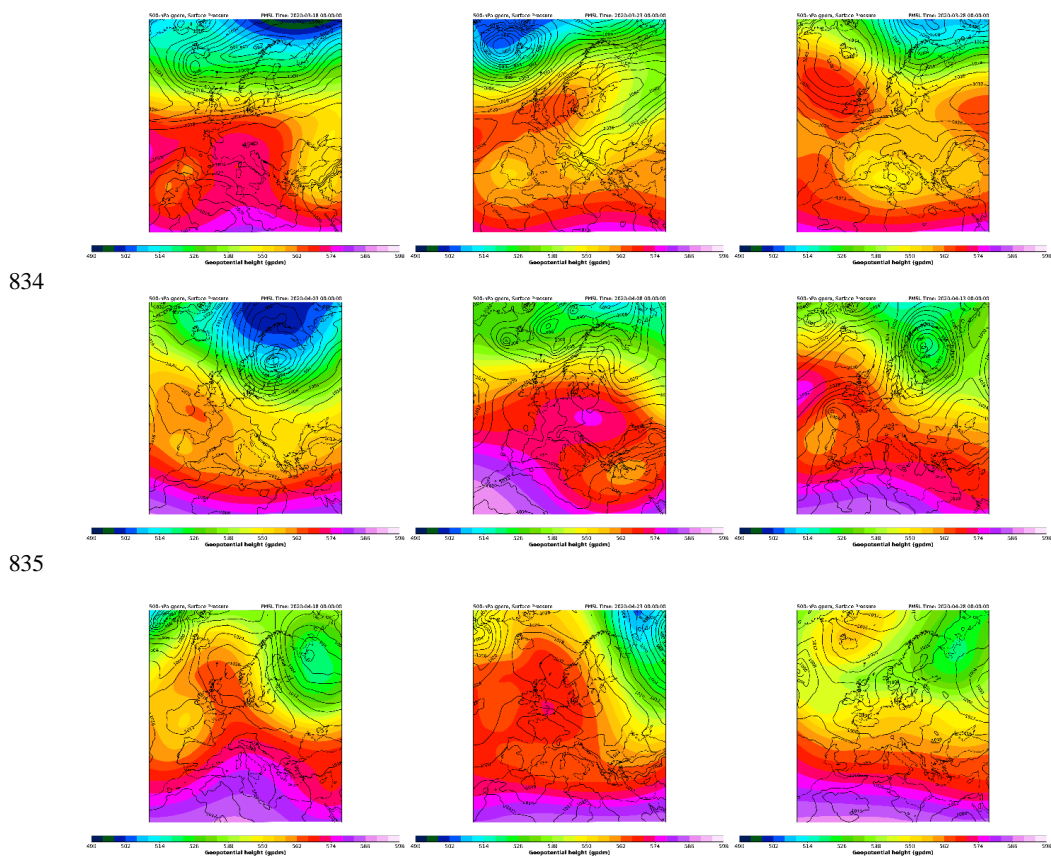
830

831

832

Figure A4: Time series of the monthly accumulated precipitation and mean solar irradiance between 10 and 14 UTC at the Wettermast Hamburg for April from 1997-2020.

833

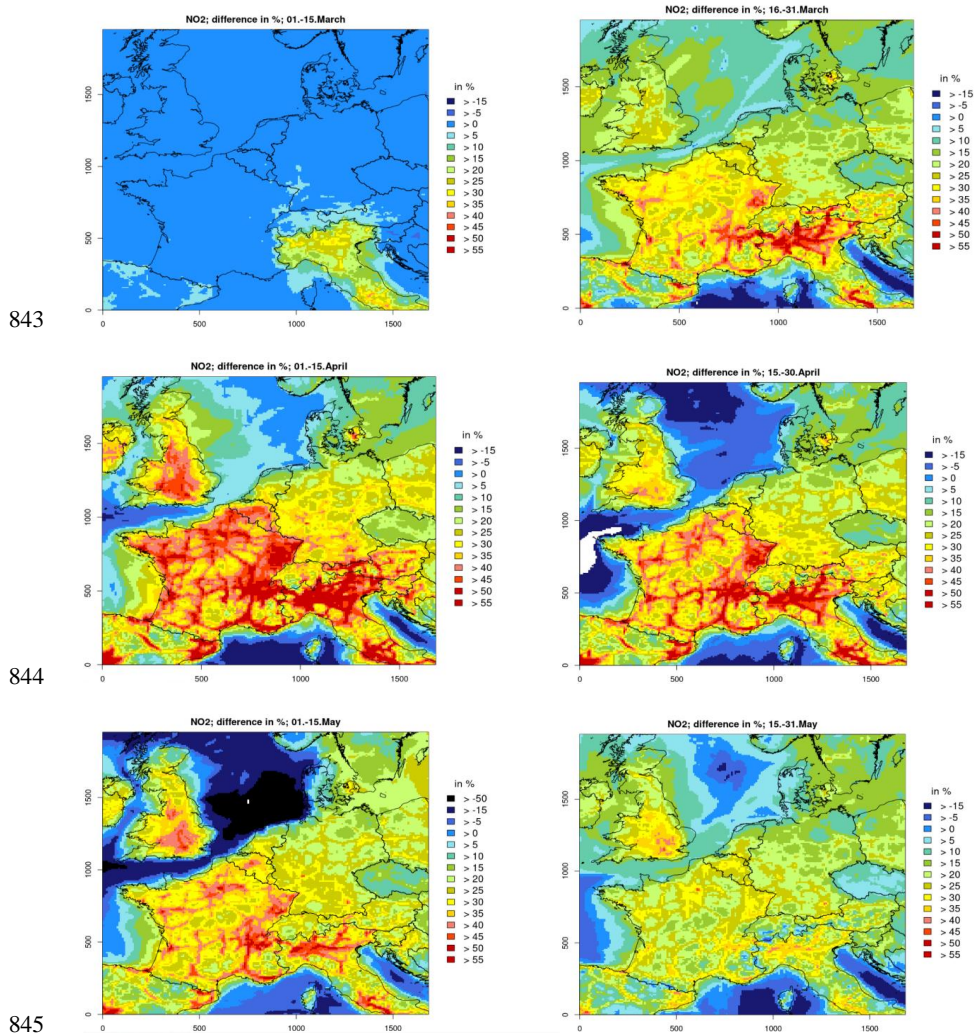


837 **Figure A5:** 500 hPa geopotential heights (in gpdm) and surface pressure (in hPa) for 4-days time segments in March
838 and April 2020 according to the COSMO simulations. The geopotential heights are averaged over 4 days, displayed
839 surface pressure distributions are representative snap shots within those time segments.

840

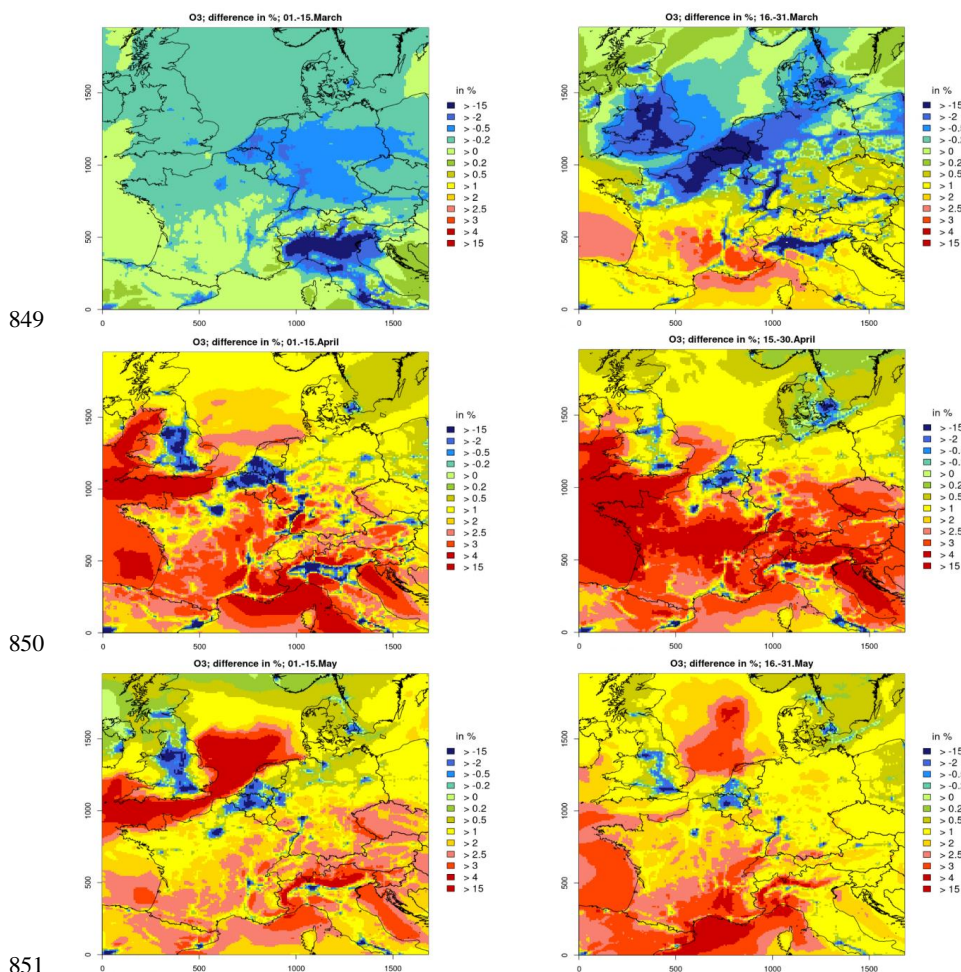
841 **A3 COVID-19 lockdown effects**

842



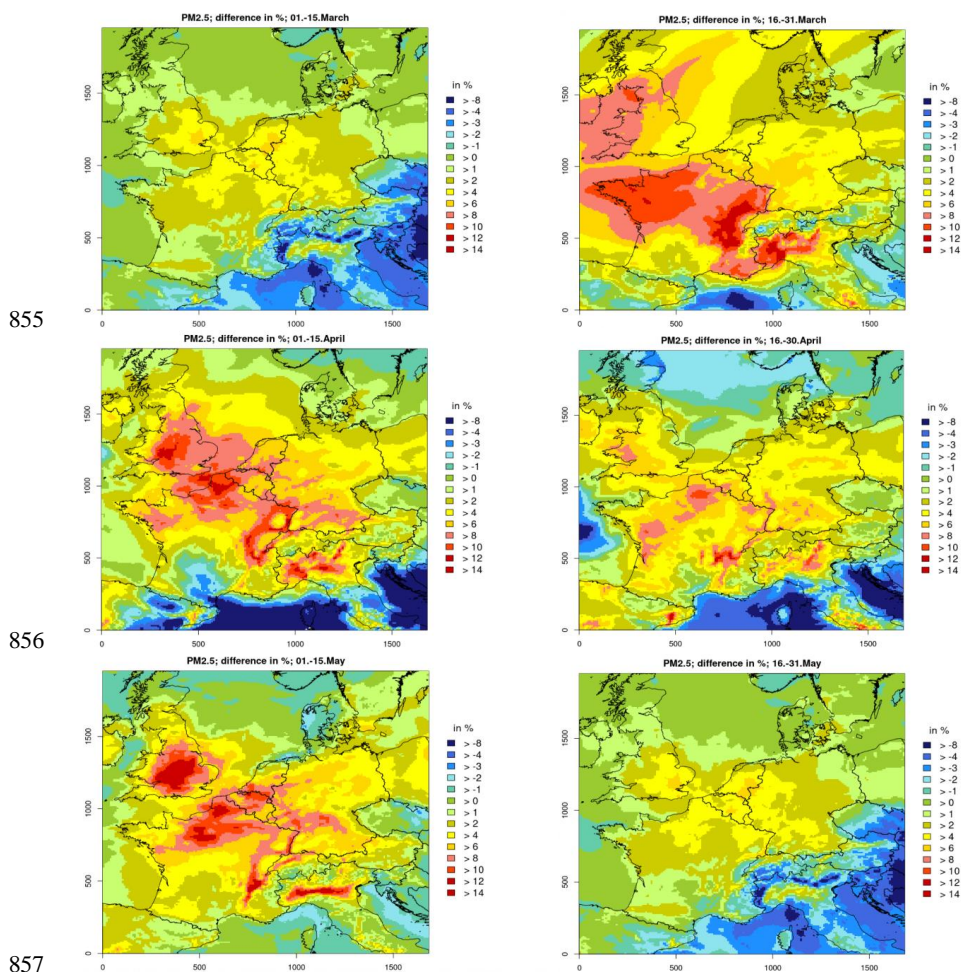
846 **Figure A6: CMAQ results for relative NO₂ concentrations reductions due to lockdown measures (noCOV – COV run)**
847 **in Central Europe between 1 March and 31 May 2020 in half-monthly intervals; positive values denote reductions.**

848



852 **Figure A7: CMAQ results for relative O₃ concentrations reductions due to lockdown measures (noCOV – COV run)**
853 **in Central Europe between 1 March and 31 May 2020 in half-monthly intervals; positive values denote reductions.**

854

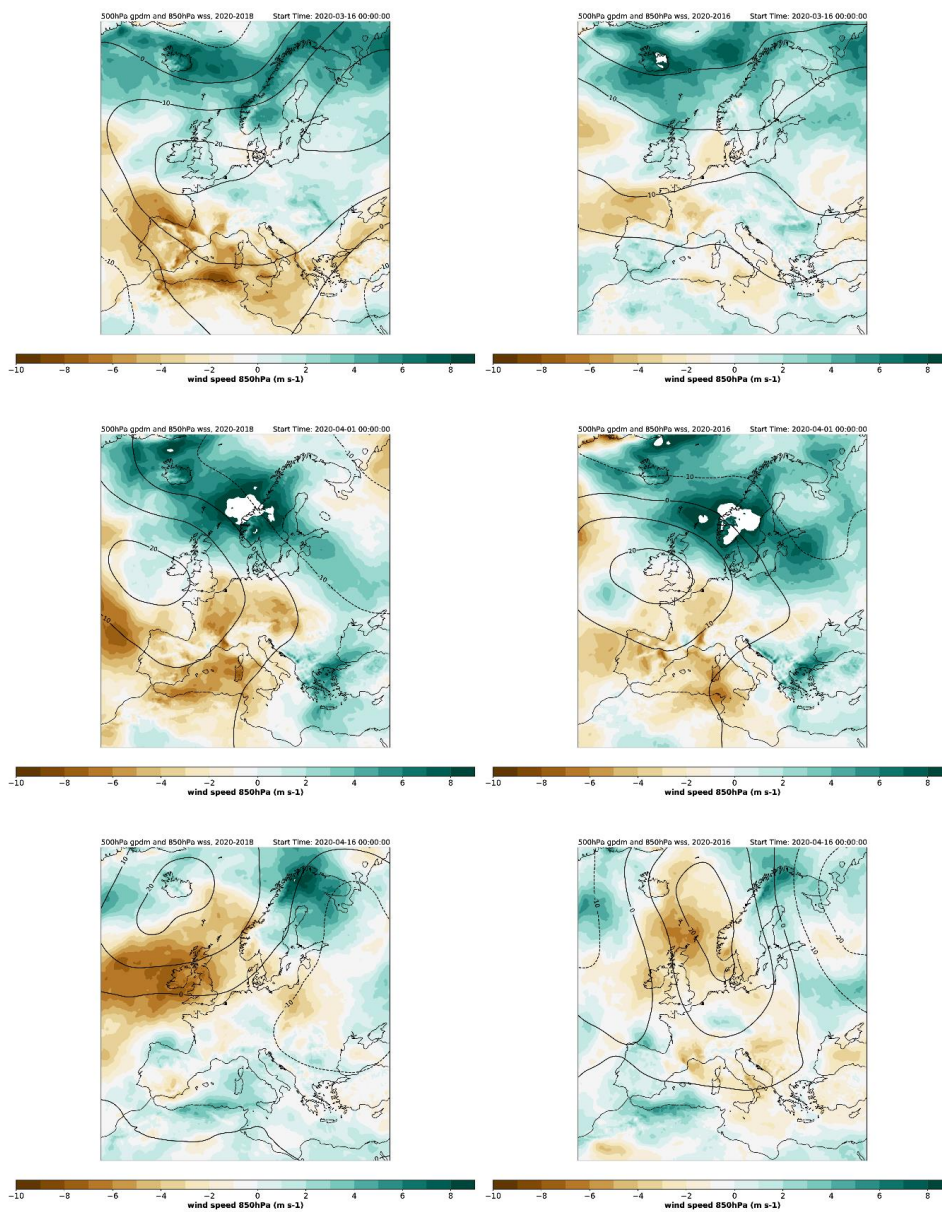


858 **Figure A8: CMAQ results for relative PM_{2.5} concentrations reductions due to lockdown measures (noCOV – COV**
859 **run) in Central Europe between 1 March and 31 May 2020 in half-monthly intervals; positive values denote reductions.**

860

861 **A4 Discussion**

862



863

864

865

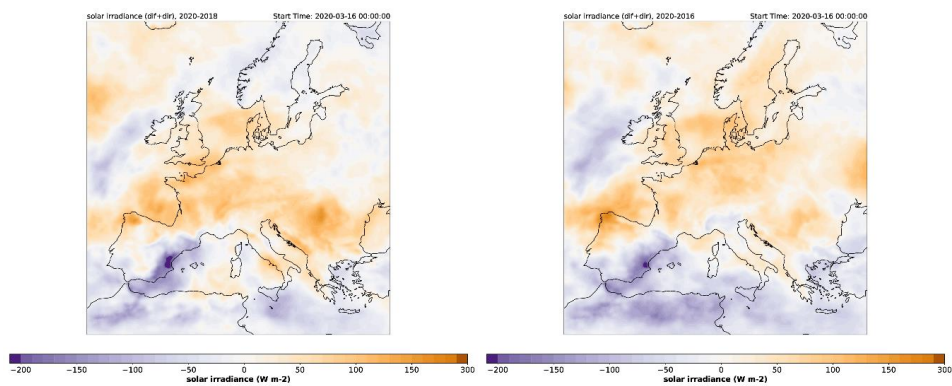
866 **Figure A9: Geopotential height at 500 hPa (in gpdm, isolines) and windspeed at 850 hPa (in m/s, color code): Differences**
867 **between 2020 and 2018 (left column) and 2020 and 2016 (right column) for the half month-periods 16 march – 31 March**
868 **(top), 1 April – 15 April (middle) and 16 April – 30 April (bottom).**

869

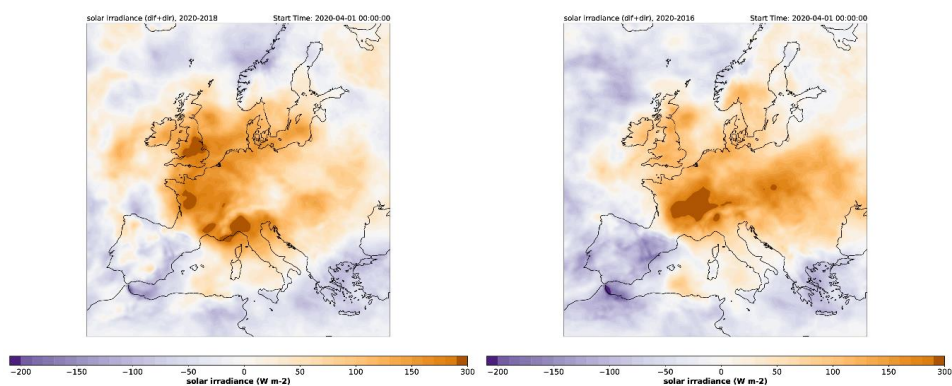
870



871



872



873

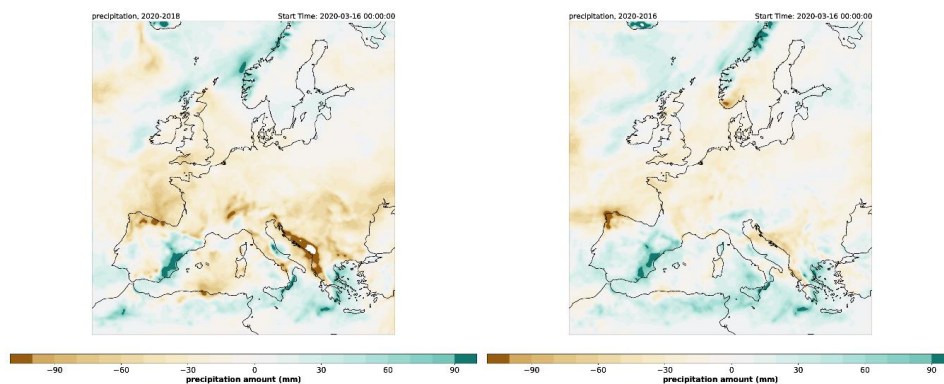
874 **Figure A10: Solar irradiance (in W/m^2 , color code): Differences between 2020 and 2018 (left column) and 2020 and**
875 **2016 (right column) for the half month-periods 16 March – 31 March (top), 1 April – 15 April (middle) and 16 April –**
876 **30 April (bottom).**

877

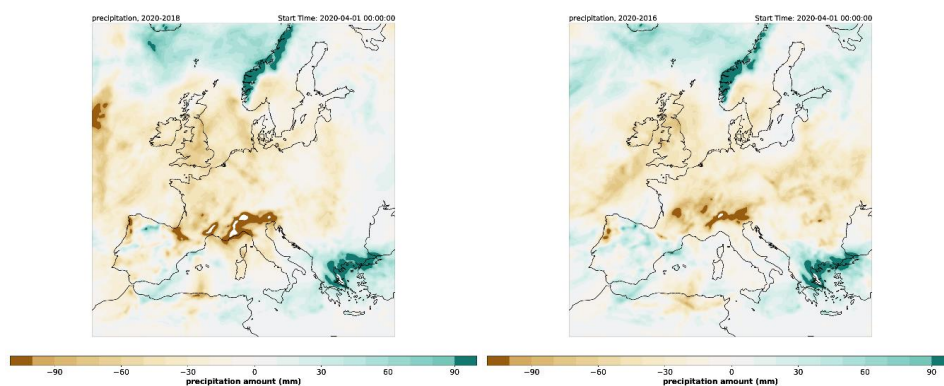
878



879



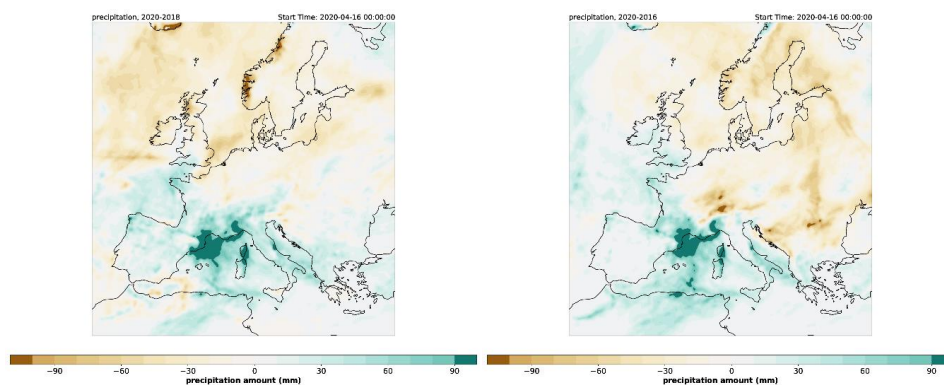
880



881

882 **Figure A11: Accumulated precipitation (in mm, color code): Differences between 2020 and 2018 (left column) and 2020**
883 **and 2016 (right column) for the half month-periods 16 March – 31 March (top), 1 April – 15 April (middle) and 16**
884 **April – 30 April (bottom).**

885





886 **References**

887

888 Amouei Torkmahalleh, M., Akhmetvaliyeva, Z., Omran, A. D., Faezeh Darvish Omran, F., Kazemitabar, M.,
889 Naseri, M., Naseri, M., Sharifi, H., Malekipirbazari, M., Kwasi Adotey, E., Gorjinezhad, S., Eghtesadi, N.,
890 Sabanov, S., Alastuey, A., de Fátima Andrade, M., Buonanno, G., Carbone, S., Cárdenas-Fuentes, D. E., Cassee,
891 F. R., Dai, Q., Henríquez, A., Hopke, P. K., Keronen, P., Khwaja, H. A., Kim, J., Kulmala, M., Kumar, P., Kushta,
892 J., Kuula, J., Massagué, J., Mitchell, T., Mooibroek, D., Morawska, L., Niemi, J. V., Ngagine, S. H., Norman, M.,
893 Oyama, B., Oyola, P., Öztürk, F., Petäjä, T., Querol, X., Rashidi, Y., Reyes, F., Ross-Jones, M., Salthammer, T.,
894 Savvides, C., Stabile, L., Sjöberg, K., Söderlund, K., Sunder Raman, R., Timonen, H., Umezawa, M., Viana, M.,
895 and Xie, S.: Global Air Quality and COVID-19 Pandemic: Do We Breathe Cleaner Air?, *Aerosol and Air Quality*
896 *Research*, 21, 200567, 10.4209/aaqr.200567, 2021.

897 Baldauf, M., Seifert, A., Forstner, J., Majewski, D., Raschendorfer, M., and Reinhardt, T.: Operational
898 Convective-Scale Numerical Weather Prediction with the COSMO Model: Description and Sensitivities, *Monthly*
899 *Weather Review*, 139, 3887-3905, 10.1175/mwr-d-10-05013.1, 2011.

900 Baret, F., Weiss, M., Lacaze, R., Camacho, F., Makhmara, H., Pacholczyk, P., and Smets, B.: GEOV1: LAI and
901 FAPAR essential climate variables and FCOVER global time series capitalizing over existing products. Part1:
902 Principles of development and production, *Remote Sensing of Environment*, 137, 299-309,
903 10.1016/j.rse.2012.12.027, 2013.

904 Bauwens, M., Compennolle, S., Stavrou, T., Muller, J. F., van Gent, J., Eskes, H., Levelt, P. F., van der, A. R.,
905 Veeffkind, J. P., Vlietinck, J., Yu, H., and Zehner, C.: Impact of coronavirus outbreak on NO₂ pollution assessed
906 using TROPOMI and OMI observations, *Geophys Res Lett*, e2020GL087978, 10.1029/2020GL087978, 2020.

907 Bieser, J., Aulinger, A., Matthias, V., Quante, M., and Builtjes, P.: SMOKE for Europe - adaptation, modification
908 and evaluation of a comprehensive emission model for Europe, *Geoscientific Model Development*, 3, 949-1007,
909 2010.

910 Bieser, J., Aulinger, A., Matthias, V., Quante, M., and Denier van der Gon, H. A. C.: Vertical emission profiles
911 for Europe based on plume rise calculations, *Environmental Pollution*, 159, 2935-2946, 2011.

912 Bissolli, P., and Dittmann, E.: The objective weather type classification of the German Weather Service and its
913 possibilities of application to environmental and meteorological investigations, *Meteorologische Zeitschrift*, 10,
914 253-260, 10.1127/0941-2948/2001/0010-0253, 2001.

915 Brümmer, B., and Schultze, M.: Analysis of a 7-year low-level temperature inversion data set measured at the 280
916 m high Hamburg weather mast, *Meteorologische Zeitschrift*, 24, 481-494, 10.1127/metz/2015/0669, 2015.

917 Byun, D., and Schere, K. L.: Review of the Governing Equations, Computational Algorithms, and Other
918 Components of the Models-3 Community Multiscale Air Quality (CMAQ) Modeling System, *Applied Mechanics*
919 *Reviews*, 59, 51-77, 2006.

920 Byun, D. W., and Ching, J. K. S.: Science Algorithms of the EPA Models-3 Community Multiscale Air Quality
921 Modeling System, 1999.

922 Collivignarelli, M. C., Abba, A., Caccamo, F. M., Bertanza, G., Pedrazzani, R., Baldi, M., Ricciardi, P., and
923 Miino, M. C.: Can particulate matter be identified as the primary cause of the rapid spread of CoViD-19 in some
924 areas of Northern Italy?, *Environmental Science and Pollution Research*, 10.1007/s11356-021-12735-x, 2020.



- 925 Denier van der Gon, H. A. C., Hendriks, C., Kuenen, J., Segers, A., and Visschedijk, A.: Description of current
926 temporal emission patterns and sensitivity of predicted AQ for temporal emission patterns EU FP7 MACC
927 deliverable report D_D-EMIS_1.3, 2011.
- 928 Doms, G., and Schättler, U.: A Description of the Nonhydrostatic Regional Model LM. Part I: Dynamics and
929 Numerics, 2002.
- 930 Doms, G., Foerstner, J., Heise, E., Herzog, H. J., Mrionow, D., Raschendorfer, M., Reinhart, T., Ritter, B.,
931 Schrodin, R., Schulz, J. P., and Vogel, G.: A Description of the Nonhydrostatic Regional COSMO Model. Part II:
932 Physical Parameterization, 2011.
- 933 Forster, P. M., Forster, H. I., Evans, M. J., Gidden, M. J., Jones, C. D., Keller, C. A., Lamboll, R. D., Quéré, C.
934 L., Rogelj, J., Rosen, D., Schleussner, C.-F., Richardson, T. B., Smith, C. J., and Turnock, S. T.: Current and
935 future global climate impacts resulting from COVID-19, *Nature Climate Change*, 10, 913-919, 10.1038/s41558-
936 020-0883-0, 2020.
- 937 Gelaro, R., McCarty, W., Suarez, M. J., Todling, R., Molod, A., Takacs, L., Randles, C. A., Darmenov, A.,
938 Bosilovich, M. G., Reichle, R., Wargan, K., Coy, L., Cullather, R., Draper, C., Akella, S., Buchard, V., Conaty,
939 A., da Silva, A. M., Gu, W., Kim, G. K., Koster, R., Lucchesi, R., Merkova, D., Nielsen, J. E., Partyka, G., Pawson,
940 S., Putman, W., Rienecker, M., Schubert, S. D., Sienkiewicz, M., and Zhao, B.: The Modern-Era Retrospective
941 Analysis for Research and Applications, Version 2 (MERRA-2), *Journal of Climate*, 30, 5419-5454, 10.1175/jcli-
942 d-16-0758.1, 2017.
- 943 Gkatzelis, G. I., Gilman, J. B., Brown, S. S., Eskes, H., Gomes, A. R., Lange, A. C., McDonald, B. C., Peischl, J.,
944 Petzold, A., Thompson, C. R., and Kiendler-Scharr, A.: The global impacts of COVID-19 lockdowns on urban
945 air pollution: A critical review and recommendations, *Elementa: Science of the Anthropocene*, 9,
946 10.1525/elementa.2021.00176, 2021.
- 947 Guenther, A., Jiang, X., Shah, T., Huang, L., S. Kemball-Cook, and Yarwood, G.: Model of Emissions of Gases
948 and Aerosol from Nature Version 3 (MEGAN3) for Estimating Biogenic Emissions, *Air Pollution Modeling and
949 Its Application XXVI*, edited by: Mensink, C., Gong, W., and Hakami, A., Springer International Publishing,
950 Cham, 187-192 pp., 2020.
- 951 Guenther, A. B., Jiang, X., Heald, C. L., Sakulyanontvittaya, T., Duhl, T., Emmons, L. K., and Wang, X.: The
952 Model of Emissions of Gases and Aerosols from Nature version 2.1 (MEGAN2.1): an extended and updated
953 framework for modeling biogenic emissions, *Geoscientific Model Development*, 5, 1471-1492, 2012.
- 954 Hess, P., and Brezowsky, H.: Katalog der Großwetterlagen Europas, Offenbach a.M., , 14 & 54, 1977.
- 955 Huang, X., Ding, A., Gao, J., Zheng, B., Zhou, D., Qi, X., Tang, R., Wang, J., Ren, C., Nie, W., Chi, X., Xu, Z.,
956 Chen, L., Li, Y., Che, F., Pang, N., Wang, H., Tong, D., Qin, W., Cheng, W., Liu, W., Fu, Q., Liu, B., Chai, F.,
957 Davis, S. J., Zhang, Q., and He, K.: Enhanced secondary pollution offset reduction of primary emissions during
958 COVID-19 lockdown in China, *National Science Review*, 10.1093/nsr/nwaa137, 2020.
- 959 Inness, A., Ades, M., Agustí-Panareda, A., Barré, J., Benedictow, A., Blechschmidt, A., Dominguez, J., Engelen,
960 R., Eskes, H., Flemming, J., Huijnen, V., Jones, L., Kipling, Z., Massart, S., Parrington, M., Peuch, V.-H., M, R.,
961 Remy, S., Schulz, M., and Suttie, M.: CAMS global reanalysis (EAC4). , in, edited by: (ADS), C. A. M. S. C. A.
962 D. S., 2019a.
- 963 Inness, A., Ades, M., Agustí-Panareda, A., Barre, J., Benedictow, A., Blechschmidt, A. M., Dominguez, J. J.,
964 Engelen, R., Eskes, H., Flemming, J., Huijnen, V., Jones, L., Kipling, Z., Massart, S., Parrington, M., Pench, V.



- 965 H., Razinger, M., Remy, S., Schulz, M., and Suttie, M.: The CAMS reanalysis of atmospheric composition,
966 Atmospheric Chemistry and Physics, 19, 3515-3556, 10.5194/acp-19-3515-2019, 2019b.
- 967 James, P. M.: An objective classification method for Hess and Brezowsky Grosswetterlagen over Europe,
968 Theoretical and Applied Climatology, 88, 17-42, 10.1007/s00704-006-0239-3, 2007.
- 969 Kelly, J. T., Bhave, P. V., Nolte, C. G., Shankar, U., and Foley, K. M.: Simulating emission and chemical evolution
970 of coarse sea-salt particles in the Community Multiscale Air Quality (CMAQ) model, Geoscientific Model
971 Development, 3, 257-273, 2010.
- 972 Kroll, J. H., Heald, C. L., Cappa, C. D., Farmer, D. K., Fry, J. L., Murphy, J. G., and Steiner, A. L.: The complex
973 chemical effects of COVID-19 shutdowns on air quality, Nat Chem, 12, 777-779, 10.1038/s41557-020-0535-z,
974 2020.
- 975 Lonati, G., and Riva, F.: Regional Scale Impact of the COVID-19 Lockdown on Air Quality: Gaseous Pollutants
976 in the Po Valley, Northern Italy, Atmosphere, 12, 264, 2021.
- 977 Matthias, V., Arndt, J. A., Aulinger, A., Bieser, J., van der Gon, H. D., Kranenburg, R., Kuenen, J., Neumann, D.,
978 Pouliot, G., and Quante, M.: Modeling emissions for three-dimensional atmospheric chemistry transport models,
979 Journal of the Air & Waste Management Association, 68, 763-800, 10.1080/10962247.2018.1424057, 2018.
- 980 Menut, L., Bessagnet, B., Siour, G., Mailler, S., Pennel, R., and Cholakian, A.: Impact of lockdown measures to
981 combat Covid-19 on air quality over western Europe, Sci Total Environ, 741, 140426,
982 10.1016/j.scitotenv.2020.140426, 2020.
- 983 Mertens, M., Jöckel, P., Matthes, S., Nützel, M., Grewe, V., and Sausen, R.: COVID-19 induced lower-
984 tropospheric ozonechanges, Environ. Res. Lett., in press, 10.1088/1748-9326/abf191, 2021.
- 985 Petetin, H., Bowdalo, D., Soret, A., Guevara, M., Jorba, O., Serradell, K., and Garcia-Pando, C. P.: Meteorology-
986 normalized impact of the COVID-19 lockdown upon NO₂ pollution in Spain, Atmospheric Chemistry and
987 Physics, 20, 11119-11141, 10.5194/acp-20-11119-2020, 2020.
- 988 Petrik, R., Geyer, B., and Rockel, B.: On the diurnal cycle and variability of winds in the lower planetary boundary
989 layer: evaluation of regional reanalyses and hindcasts, Tellus Series a-Dynamic Meteorology and Oceanography,
990 73, 1-28, 10.1080/16000870.2020.1804294, 2021.
- 991 Rockel, B., Will, A., and Hense, A.: The Regional Climate Model COSMO-CLM(CCLM), Meteorologische
992 Zeitschrift, 17, 347-348, 2008.
- 993 Schwarzkopf, D. A., Petrik, R., Matthias, V., and Quante, M.: A Ship Emission Modeling System with Scenario
994 Capabilities, Geoscientific Model Development, in preparation, 2021.
- 995 Sharma, S., Zhang, M., Anshika, Gao, J., Zhang, H., and Kota, S. H.: Effect of restricted emissions during COVID-
996 19 on air quality in India, Sci Total Environ, 728, 138878, 10.1016/j.scitotenv.2020.138878, 2020.
- 997 Solazzo, E., Bianconi, R., Pirovano, G., Matthias, V., Vautard, R., Moran, M. D., Appel, K. W., Bessagnet, B.,
998 Brandt, J., Christensen, J. H., Chemel, C., Coll, I., Ferreira, J., Forkel, R., Francis, X. V., Grell, G., Grossi, P.,
999 Hansen, A. B., Miranda, A. I., Nopmongcol, U., Prank, M., Sartelet, K. N., Schaap, M., Silver, J. D., Sokhi, R. S.,
1000 Vira, J., Werhahn, J., Wolke, R., Yarwood, G., Zhang, J., Rao, S. T., and Galmarini, S.: Operational model
1001 evaluation for particulate matter in Europe and North America in the context of AQMEII, Atmospheric
1002 Environment, 53, 75-92, 2012.
- 1003 van Heerwaarden, C. C., Mol, W. B., Veerman, M. A., Benedict, I., Heusinkveld, B. G., Knap, W. H., Kazadzis,
1004 S., Kouremeti, N., and Fiedler, S.: Record high solar irradiance in Western Europe during first COVID-19



1005 lockdown largely due to unusual weather, *Communications Earth & Environment*, 2, 37, 10.1038/s43247-021-
1006 00110-0, 2021.
1007 Velders, G. J. M., Willers, S. M., Wesseling, J., den Elshout, S. v., van der Swaluw, E., Mooibroek, D., and van
1008 Ratingen, S.: Improvements in air quality in the Netherlands during the corona lockdown based on observations
1009 and model simulations, *Atmospheric Environment*, 247, 10.1016/j.atmosenv.2020.118158, 2021.
1010